THERYA, 2020, Vol. 11(3):508-532 DOI:10.12933/therya-20-999 ISSN 2007-3364

A new bat species of the genus *Myotis* with comments on the phylogenetic placement of *M. keaysi* and *M. pilosatibialis*

Carlos Alberto Carrión-Bonilla[1, 2*], and Joseph Anthony Cook[1]

[1] Department of Biology and Museum of Southwestern Biology, University of New Mexico. Albuquerque, NM 87131, USA. Email:ccarrion@unm.edu, lophostoma1@gmail.com (CACB), tucojoe@gmail.com (JAC).

[2] Museo de Zoología. Escuela de Ciencias Biológicas. Pontificia Universidad Católica del Ecuador. Av. 12 de Octubre y Roca, Apartado 17-01-2184. Quito, Ecuador. Email:ccarrion@unm.edu, lophostoma1@gmail (CAC-B).

*Corresponding author

Molecular studies of Neotropical *Myotis* (Chiroptera, Vespertilionidae) in the last decade have uncovered substantial cryptic diversity. One example is *M. keaysi pilosatibialis*, which is characterized by a complex taxonomy derived from low morphological variation. Herein, we studied cryptic diversity of a high elevation clade from premontane and montane forest of Chiriquí Province (Panamá), Cordillera Oriental (Ecuador), and Valle del Silencio (Costa Rica). Additionally, we disentangle relationships of *M. k. keaysi* and *M. k. pilosatibialis* by determining their phylogenetic placement within the Neotropical *Myotis* radiation. In the process, we identified a new lineage of species level hierarchy that is described herein. We used an integrative taxonomy approach, using a combination of linear morphometrics, qualitative morphology, molecular phylogenetics, and climatic analysis. The newly identified lineage is a sister species to *M. pilosatibialis str.,* but differs from *M.* sp. (Quintana Roo, México), *M. keaysi str.*, and *M. oxyotus gardneri* in size and other quantitative morphological characters in addition to both nuclear and mitochondrial DNA sequence divergence. Based on our phylogenetic analysis of partial cytochrome *b* sequence, the polyphyly of *M. keaysi str.* and *M. pilosatibialis str.* is resolved, with *M. keaysi str.* paraphyletic to *M. ruber* and *M. simus*. *Myotis pilosatibialis* is part of a monophyletic clade that is sister to the newly identified species. This report refines our understanding of taxonomy and systematics of the *Myotis pilosatibialis* complex of bats, identifies and describes a new species of *Myotis,* and more broadly it contributes to efforts to characterize species in this genus in Neotropical environments. Based on its distribution, we classified this newly described species as paramontane due to its restriction to premontane and montane forest of Chiriquí Province (Panamá), Valle del Silencio (Costa Rica), and Cordillera Oriental (Ecuador). These habitats are susceptible to the effects of climate change, in addition to ongoing habitat destruction.

Los estudios de genética molecular del género de murciélagos Neotropicales *Myotis* (Chiroptera: Vespertilionidae) han permitido descubrir diversidad críptica en la última década. Un ejemplo es *M. keaysi pilosatibialis*, el cual se caracteriza por una taxonomía compleja con poca variabilidad morfológica. En esta investigación, estudiamos un clado de murciélagos myotinos de los bosques premontanos y montanos de la Provincia de Chiriquí (Panamá), Cordillera Oriental (Ecuador) y el Valle del Silencio (Costa Rica). Adicionalmente, resolvemos las relaciones de *M. k. keaysi* y *M. k. pilosatibialis* al determinar su posición filogenética en la radiación de *Myotis* en el Neotrópico. En el proceso, identificamos una entidad biológica a nivel de especies que es descrita es esta contribución. Desde un enfoque de taxonomía integrativa, utilizamos una combinación de morfometría lineal, caracteres morfológicos cualitativos, así como análisis filogenéticos moleculares y de clima. La nueva especie es evolutivamente cercana a *M. pilosatibialis str,* pero difiere de *M.* sp. (Quintan Roo, México), *M. keaysi str.* y *M. oxyotus gardneri* por su tamaño y otros caracteres morfológicos cuantitativos, así como divergencia evolutiva en secuencias de genes mitocondriales y nucleares. Con base a nuestro análisis filogenético del fragmento parcial del gen citocromo *b*, resolvemos las relaciones polifiléticas de *M. keaysi str.* y *M. pilosatibialis str. Myotis keaysi str.* es parafilético en relación con *M. ruber* y *M. simus*. *M. pilosatibialis str.* forma parte de un clado monofilético hermano a este nuevo linaje. Este trabajo contribuye a refinar la taxonomía y sistemática del complejo de especies *Myotis pilosatibialis*, identifica y describe una especie nueva de *Myotis*, así como aporta de una manera más amplia a los esfuerzos de caracterizar especies de este género en ambientes neotropicales. Basado en su distribución geográfica, este nuevo clado de murciélagos myotinos se clasifica como paramontano, debido a su distribución a bosques premontanos y montanos de los Chiriquí (Panamá), Valle del Silencio (Costa Rica) y Cordillera Oriental (Ecuador). Estos hábitats son susceptibles a los efectos del cambio climático y la continua destrucción del mismo.

Keywords: Armien's *Myotis*; Chiriquí province; Cordillera Oriental; cryptic diversity; *Myotis armiensis*; Neotropics; Valle del Silencio.

Introduction

Bats of the widely distributed genus *Myotis* are an excellent model for studies of diversification and historical biogeography (Stadelmann *et al.* 2007; Ruedi *et al.* 2013). With *ca.* 134 species (www.mammaldiversity.org), *Myotis* is one of the more remarkable mammalian radiations worldwide. Although long considered to be a classic example of an adaptive radiation in temperate regions, more detailed studies of Neotropical (Larsen *et al.* 2012a, b) and Afrotropical species (Patterson *et al.* 2019) using molecular data are now uncovering substantial cryptic diversity (Bickford *et al.* 2007) in tropical regions.

Based on previous systematic revisions (La Val 1973; Hernandez-Meza *et al.* 2005; Wilson 2008; Moratelli and Wilson 2014; Mantilla-Meluck and Muñoz-Garay 2014), the nominal species *M. keaysi* was partitioned into two

subspecies: *M. k. keaysi* J. A. Allen 1914, distributed in the Andes of Colombia, Colombian Caribbean, Perú, Ecuador, Bolivia, and Argentina above 1,100 m, with most specimens known from above 2,000 m and *M. k. pilosatibialis* (La Val 1973), occurring in northern Venezuela, the island of Trinidad, Colombian Caribbean, eastern cordillera of the Colombian Andes, and elsewhere from southern México, southeastward through Central America into northwestern Panamá. Both subspecies are known to occur in sympatry in Caribbean Colombia and the eastern cordillera of Colombia. Although the phylogenetic placement for both is still pending, Mantilla-Meluck and Muñoz-Garay (2014) recognized *pilosatibialis* as distinct at the species level based on morphology. Based on those findings, Moratelli and Wilson (2014) recommended reassigning the specimens previously assigned to *M. keaysi* by Stadelmann *et al.* (2007) and Ruedi *et al.* (2013) from Yucatán (México) to *M. pilosatibialis*. Furthermore, Moratelli *et al.* (2016) and Moratelli *et al.* (2017) were unable to confidently identify these specimens from Yucatán, México and assigned provisionally a "cf ." (Latin, confer), preceding the specific epithet.

Myotis keaysi as envisioned by Stadelmann *et al.* 2007 and Ruedi *et al.* 2013 was identified as a monophyletic clade with considerable geographic structure and at least three different lineages (Larsen *et al.* 2012a; Chaverri *et al.* 2016), which were named as follows: *M. keaysi* (Yucatán Peninsula, México), *M.* cf. *keaysi* 2 (México, El Salvador, Guatemala), and an unnamed clade from the mountain tops of Cordillera Oriental from Ecuador and Panamá (Clare *et al.* 2011; Larsen *et al.* 2012b) that was later suggested to be *M. keaysi* (Costa Rica) in Chaverri et al. (2016).

In this study, we provided the phylogenetic placement for *M. keaysi str.* and *M. pilosatibialis str.* in the *Myotis* Neotropical radiation and under this phylogenetic framework, we reviewed specimens from the unnamed clade from mountain tops of Chiriquí (Panamá) and Cordillera Oriental (Ecuador). We found that these specimens are distinct from other species of Neotropical *Myotis* and described this new species based on the General Lineage Concept (GLC), which uses the concept of species as separately evolving metapopulation lineages that can be recognized using diverse secondary recognition criteria (De Queiroz 2007). We apply the criteria used by Florio *et al.* (2012) as follows: a) identify lineages based on clades from analysis of multiple molecular markers b) employ multivariate procedures such as principal component analysis (PCA) and discriminant function analysis (DFA) to determine morphological variation associated with these phylogenetic groups, and c) use climatic analysis to evaluate the environment and geographic space occupied by the groups supported by covariation of genetic and morphological evidence.

Methods

Specimens in Panamá were collected under an ongoing project entitled "Caracterización de la epidemiología y ecología de enfermedades zoonóticas trasmitidas por vectores (emergentes y reemergentes) en áreas silenciosas y conocidas de Panamá" signed by Instituto Conmemorativo Gorgas and Ministerio del Medio Ambiente de Panamá, with permits SC/A-50-1 and SEX/A-1-19. In Ecuador, specimens were collected under the project "Caracterización de la diversidad biológica y genética de los mamíferos del Ecuador", signed by Pontificia Universidad Católica del Ecuador and Ministerio del Medio Ambiente (MAE), with permits (MAE-DNB-CM-2016-004 and 70-12-2017- DPAN/MAE). Specimens in both countries were collected with ground-level mist netting and field methods generally followed Galbreath *et al.* (2019), under guidelines of the American Society of Mammalogists (Sikes *et al.* 2016) and approved by the University of New Mexico Animal Care and Use Committee.

Specimens examined. Specimens directly examined ($n = 72$) for this research include representatives of Central and South American *Myotis*, including type specimens (Appendix I). These comprise fluid-preserved specimens, stuffed skins, and skulls deposited in the following institutions: American Museum of Natural History (AMNH); Field Museum of Natural History, Chicago (FMNH); Natural History Museum, University of Kansas (KU); Natural History Museum of Los Angeles County, Los Angeles (LACM); Louisiana State University Museum of Natural Science (LSUMZ); Museum of Vertebrate Zoology, University of California, Berkeley (MVZ); Museum of Southwestern Biology, University of New Mexico (MSB); National Museum of Natural History, Smithsonian Institution (USNM); Museo de Zoología, División de Mastozoología, Pontificia Universidad Católica del Ecuador (QCAZ); Royal Ontario Museum (ROM); Sam Noble Oklahoma Museum of Natural History, University of Oklahoma (SNOMNH); Texas A&M Biodiversity Research and Teaching Collection, College Station (TCWC); Museum of Texas Tech University (TTU; Dunnum *et al.* 2018). These specimens were identified according to Wilson (2008), Moratelli and Wilson (2011), Moratelli *et al.* (2013), Moratelli *et al.* (2017).

Measurements. All measurements are in millimeters (mm) or grams (body mass) and are from adults. The lengths of head and body (HB), tail, hind foot, ear, and the body weight (mass) were recorded from skin labels and are reported to the nearest millimeter or nearest gram. Forearm length (FA) and third metacarpal length (3ML) were directly measured from specimens. Measurements were taken using digital calipers accurate to 0.02 mm. Craniometric measurements were taken under a binocular microscope at low magnification (usually 6x). These dimensions were recorded and analyzed to the nearest 0.01 mm, but values were rounded off to 0.1 mm throughout the text because this is the smallest unit allowing accurate repeatability with calipers (Voss *et al.* 2013).

Measurements include four external, 14 cranial, and two mandibular dimensions. The measurements and abbreviations are defined as follows: forearm length (FA), from the elbow to the distal end of the forearm including car-

pals; third metacarpal length (3ML), from the distal end of the forearm including carpals to the distal end of the third metacarpal; length of dorsal hairs (LDH), from the base to the tip of the hair in the fur between the scapulae; length of ventral hairs (LVH) in fur at mid thorax; greatest length of the skull (GLS), from the apex of the upper internal incisors to the occiput; condylocanine length (CCL), from the anterior surface of the upper canines to a line connecting the occipital condyles; condylobasal length (CBL), from the premaxillae to a line connecting the occipital condyles; incisive length (CIL), from the apex of upper internal incisors to a line connecting the occipital condyles; basal length (BAL), from the apex of upper internal incisors to the ventral margin of the foramen magnum; zygomatic breadth (ZB), greatest breadth across the outer margins of the zygomatic arches; mastoid breadth (MAB) greatest breadth across the mastoid region (MAB); braincase breadth (BCB), greatest breadth of the globular part of the braincase; interorbital breadth (IOB), least breadth between the orbits; postorbital breadth (POB), least breadth across frontal posterior to the postorbital bulges; breadth across canines (BAC), greatest breadth across outer edges of the crowns of upper canines, including cingulae; breadth across molars (BAM), greatest breadth across outer edges of the crowns of upper molars; maxillary toothrow length (MTL), from the upper canine to M3; molariform toothrow length (M1-3), from M1 to M3; mandibular length (MAL), from the mandibular symphysis to the condyloid process; and mandibular toothrow length (MAN), from the lower canine to m3. Measurements and abbreviations are further defined in Moratelli *et al.* (2013). Descriptive statistics (mean and range) were calculated for all dimensions. The cranial index (CRI= (((IOB + BCB) x GLS)/2)) and a modification of the maxillary index (MXI = (((BAC + BAM) x MTL)/2)) were as used by Baud and Menu (1993) and López-González *et al.* (2001). We used capitalized colors from (Ridgway 1912).

Principal component analysis (PCA) and discriminant function analysis (DFA) were used to examine overall patterns of skull size and shape variation among samples. We selected the following cranial dimensions representing different axes of length and width of the skull, rostrum and mandible: GLS, CCL, CBL, CIL, BAL, MAB, BCB, IOB, POB, BAC, BAM, MTL, M1-3, MAL, MAN. To obtain a more balanced design for multivariate analysis, we selected a minimum of 4 and maximum of 10 adult specimens, totaling 33 individuals (17 females and 16 males). Males and females were pooled together to enhance analysis. PCA was used to summarize trends in size and shape variation (total data set was considered a unique sample). We conducted a varimax rotation of the loading matrix after PCA in order to have more interpretable factors with a simpler structure that can be obtained using orthogonal rotations. We used rotated PCA scores to test for statistical significance of difference among species. This was assessed by multiple analysis of variance MANOVA, with Pillai's Trace. This previous analysis was followed by one-way ANOVA. A post-hoc multiple comparison Bonferroni corrected approach was used to evaluate pairwise differences among species (Rice1989).

DFA was used to assess craniometric characters that best discriminate samples, with a priori identification of samples (Moratelli *et al.* 2013). For DFA, probabilities for misclassification rates were also assessed and individuals were resigned using a jackknife procedure. Missing data values were estimated using Amelia R package (0 % of total data set) from raw data set (Honaker *et al.* 2011). We checked for normality assumptions and measurements were log transformed (Zar 1998). Finally, variance-covariance matrices were computed using all variables.

Statistical analyses were performed in software R (R Core Team 2020). We used the following R packages as follows: MASS (DFA analysis), stats (PCA analysis), ggplot2 and ggord (graphics and visualization), factoextra (eigenvalues extraction), psych (varimax rotation), car (MANOVA analysis), rstatix (summary statistics, T-test, ANOVA, adjust P-values for multiple comparisons, formatting and adding significant symbols; Venables and Venables and Ripley 2002; Wickham 2016; Beck 2017; Fox and Weisberg 2019; Revelle 2020; Kassambara 2020; Kassambara and Mundt 2020.

We contrasted the skull size and shape of *M*. sp. n. (*n* = 10) from Chiriquí (Panamá) and Cordillera Oriental (Tungurahua Province, Ecuador); *M. pilosatibialis str.*, including the holotype specimen (*n* = 8); *M. keaysi str.* from Puno and Cuzco, Perú (*n* = 5); *M. oxyotus. gardneri*, including the holotype specimen (*n* = 6) from Costa Rica and Panamá; and specimens provisionally labelled as *M.* cf. *pilosatibialis* (*n* = 4) from Quintana Roo, Yucatán Peninsula, México, hereafter called *M*. sp. We included *M. pilosatibialis str.* (El Salvador, Guatemala, Honduras and México) and *M*. sp. (Quintana Roo, Yucatán, México) due to its close morphological similarity and phylogenetic proximity (Larsen *et al.* 2012a; Moratelli *et al.* 2016; Moratelli *et al.* 2017). Similarly, we included specimens that morphologically match *M. oxyotus gardneri* La Val 1973, which was recorded in syntopy with the newly identified lineage at Chiriquí Province (Panamá) and Valle del Silencio (Costa Rica). Likewise, we included *M. keaysi str.* from Perú, due to resemblance in external dimensions, cranial morphology and fur traits. Qualitative traits employed here to characterize and distinguish species follow Moratelli *et al.* (2013). Capitalized color nomenclature follows Ridgway (1912).

DNA Extraction, Sequencing, Editing, and Assembly of partial cytochrome b and nuclear genes. To obtain DNA sequence data, whole DNA was extracted from liver, muscle or wing tissues, following a guanidinium isothiocyanate extraction protocol, E.Z.N.A. Tissue DNA Kit (Omega), and DNeasy Blood & Tissue Kit (Qiagen). Samples were quantified using Nanodrop® ND-1000 (NanoDrop Technologies, Inc) or Qubit fluorometer kit (Invitrogen), resuspended and diluted to 25 ng/ul in ddH_2O prior to amplification.

We relied on different primers and PCR protocols, which are reported as follows: cytochrome *b* in Hoffmann and Baker

(2001); Larsen *et al.* (2012b); and Naidu *et al.* (2012); nuclear exon and intron genes in Matthee and Davis (2001); Eick *et al.* (2005); Larsen *et al.* (2012b); Lack *et al.* (2010); Roehrs *et al.* (2010); and Salicini *et al.* (2011). We targeted ~ 710 bp of cytochrome-*b* sequence (*n* = 11), 1, 038 bp of nuclear exon, (RAG2) recombination activating gene II sequence (*n* = 13), and intron region of other 3 genes, 402 bp of protein kinase C, iota sequence (PRKCI, *n* = 14), 414 bp signal transducer and activator of transcription 5A sequence (STAT5A, *n* = 14), and 475 bp of thyrotropin sequence (THY, *n* = 14). Sequencing was conducted using Applied Biosystems 3110 Sequencer of the molecular biology facility at the University of New Mexico (UNM). In Ecuador, successful amplified PCR products were sent for sequencing to the commercial laboratory Macrogen Inc in Seoul, South Korea. Editing and assembly of sequences were performed with Geneious Prime (BioMatters Ltd. 2020).

DNA Extraction and Sequencing of cytochrome oxidase c subunit I. We retrieved partial sequences of cytochrome *c* oxidase subunit I (657 bp) from mitochondrial genomes for the following species: *M. oxyotus gardneri* (*n* = 1), *M. pilosatibialis str.* (*n* = 2), *M.* sp. (*n* = 1, Quintana Roo, Yucatán, México), and *M.* sp. n. (*n* = 2). DNA was extracted using standard manual extraction methods such as DNeasy Blood & Tissue Kit (QUIAGEN, Hilden, Germany) following manufacturers guidelines, as well as one open method based on magnetic particle using KingFisher™ Duo (Thermo Fisher Scientific). DNA was incorporated into double stranded DNA short fragment libraries built following BEST protocol (Mak *et al.* 2017; Carøe *et al.* 2018) using BGISEQ-500 adapters. Libraries were sequenced using 100 base paired end read chemistry on a BGISEQ-500 sequencer machine (BGI-Copenhagen).

Mitogenomes assembly and annotation. Low quality base reads, missing bases and adapters were trimmed followed by adapters removal using Adapter Removal v2 (Lindgreen 2012; Schubert *et al.* 2016). We built mitochondrial genomes using NOVOPlasty (Dierckxsens *et al.* 2017) using as reference the mitochondrial genome of *Myotis lucifugus* accession number (NC_029849.1). Furthermore, annotation was carried on with MitoZ (Meng *et al.* 2019).

DNA Alignments and *Phylogenetic analysis.* Alignments of sequences were performed with Geneious Prime (BioMatters Ltd. 2020), using MUSCLE (Edgar 2004). Phylogenetic analysis of mitochondrial and nuclear sequences was conducted with newly generated sequences and sequences retrieved from GenBank for Neotropical species of *Myotis* previously known to form a monophyletic clade (Ruedi *et al.* 2013). We included previously generated sequences from GenBank for cytochrome-*b* for 91 individuals (Ruedi and Mayer 2001; Kawai *et al.* 2003; Rodriguez and Ammerman 2004; Stadelmann *et al.* 2004; Kawai *et al.* 2006; Stadelmann *et al.* 2007; Baird *et al.* 2008; Larsen *et al.* 2012a, b; Patterson *et al.* 2019), including unpublished data by Parlos *et al.* (2008); COXI for 51 individuals used in Chaverri *et al.* (2016); RAG2 for 14 individuals; PRKCI for 13 individuals; STAT5A for 13 individuals; and THY for 14 individuals (Lack *et al.* 2010; Roehrs *et al.* 2010)

Outgroup selection. For cytochrome *b* phylogeny, we selected three sequences of *M. gracilis*, one sequence of *M. brandtii* and one sequence of *M. yanbarensis*, which are sister species to Neotropical *Myotis*. For our cytochrome *c* oxidase subunit I phylogeny, four sequences of *M. brandtii*, and one sequence of *M. lucifugus* were used. In our species tree analysis, we included myotine bats from the Nearctic clade as well, therefore we selected the eastern Palearctic lineage *M.* cf. *ikonnikovi* as the outgroup.

Maximum likelihood trees were generated using IQ-TREE with 100 bootstraps and 1000 replicates (Nguyen *et al.* 2015; Trifinopoulos *et al.* 2016). We used the program ModelFinder (Kalyaanamoorthy *et al.* 2017) with Bayesian information criteria (BIC) for selecting a nucleotide substitution model for cytochrome-*b*, cytochrome oxidase *c* subunit I, exon and intron regions. Heterozygous nuclear introns alleles were statistically resolved using PHASE 2.1.1 (Stephens *et al*. 2001) prior to the inclusion in further analyses. We used SEQPHASE web server (Flot, 2010) to generate the input files for PHASE. The Bayesian analysis was conducted in MrBayes v.3.2 for partial cytochrome *b* and cytochrome *c* oxidase subunit I (Ronquist *et al.* 2012). The search started with a random tree and the Markov chain was run for 10 million generations with trees sampled every 1,000 generations in two replications. Default values were kept for the "*relburning*" and "*burninfrac*" options in MrBayes, therefore the first 25.000, 00 generations were discarded as burn in, and posterior probability estimates of all model parameters were based on the remaining trees. Tree convergence and stationary was accessed in the Bayesian analysis by plotting the likelihood values in Tracer v1.7.1 (Rambaut *et al.* 2018).

We follow Moratelli *et al.* (2017) when designating nodal support in the mitochondrial gene trees; for ML analyses there is a strong support for bootstraps values above ≥ 75 %, moderate support for values > 50 % and < 75 %; and negligible for support for values ≤ 50 %. For the BI analysis, there are two categories, with significant support in cases in which a node posterior probability was ≥ 0.95, and insignificant or negligible support for posterior probability values < 0.95.

Identification of molecular synapomorphies. For the identification of unique molecular synapomorphies for the newly identified lineage, we generated maximum parsimony trees from mitochondrial data sets and intron regions of 3 nuclear genes using PAUP* (Swofford 2003). For these analyses, characters were treated as unordered and equally weighted. We performed a heuristic search with random addition of sequences and tree bisection-reconnection branch swapping. We set maxtree limit to 1000, with the goal of applying a maxtree limit of 100 to each 10 random addition sequence replicate. To measure clade support, 1000 bootstrap replicates were performed on a 50 % majority-rule consensus tree. We used the command *describet-*

rees and *apolist* with delayed transformation (DELTRAN) to obtain a list of molecular synapomorphies. To polarize character state transformation, we used outgroups previously used in maximum likelihood and Bayesian analyses.

Genetic distances. We calculated K2P distances (these were computed for comparisons with previous molecular studies on Neotropical *Myotis*; *e. g*, Larsen *et al.* 2012a, b) expressed as percentages and pairwise genetic distances using uncorrected sequence divergence (*p*-distances), and modeled in MEGAv10.17 (Kumar *et al.* 2016) for mitochondrial genes.

Species tree and species delimitation. Under the multispecies coalescent model, we inferred both species tree and species delimitation. For species tree inference we used *BEAST (Heled and Drummond 2010) method using the software suite available in BEAST 2.6.2 (Bouckaert *et al.* 2019). We used three phased intron and one exon alignments with substitution, clock, and tree models unlinked among all loci. All loci were assigned the log-normal relaxed-clock model using a Yule prior and linear with constant root population size model. We decided not to include mtDNA, due to its potentially strong influence on species tree inference given its higher variability and that assumptions of lower ploidy are not always met (which is modelled by *BEAST; McLean *et al.* 2016). We ran the analysis for 1 x 10^8 generations in two replicates, saving the results every 10,000 generations. The first 10 % of each run was discarded as burn-in and assembled using LOGCOMBINER v.1.10.4 to produce a maximum clade credibility tree in TREEANNOTATOR v1.10.4. Likewise, we used Tracer v.1.7.1 to access convergence and stationarity of model parameters based on ESS values and examination of tree files.

We used STACEY v1.2.1 (Species Tree and Estimation classification, Yarely), implemented in BEAST 2.6.2 (Jones 2017; Bouckaert *et al.* 2019). This method requires no prior assignment of individual to species, and no guided tree. We ran the analysis for 2 x 10^8 generations in two replicates. After completion, we used Species Delimitation Analyzer (Jones 2015) to process log files and find the distribution over species assignments under two collapse height priors (collapse 0.0001 and 0.0005). Tracer v.1.7.1 was used to assess convergence and stationarity of model parameters based on ESS values and examination of tree files. All newly generated sequences were deposited in GenBank with accession numbers MW025265-MW025275 and MW041968 - MW042028; (see Appendix II for cytochrome *b* sequences, Appendix III for cytochrome *c* oxidase subunit *I* and Appendix IV for nuclear sequences, including previously generated ingroup and outgroup sequences used in this study).

Climatic analysis. Species climatic envelopes have been used for establishing species boundaries in cryptic species (Florio *et al.* 2012). To evaluate climatic differences among species that are closely related to *Myotis* sp. n., we only included specimens used in phylogenetic analysis (*n* = 19). We extracted values for 19 climatic variables in WorldClim at 2.5 arc second resolution (Fick and Hijmans 2017). Prior to conduct PCA analysis, we carried out a Pearson´s correlation analysis to indicate presence of multicollinearity among climatic variables. Based on this analysis, we selected nine bioclimatic variables as follows: BIO1 = Annual Temperature, BIO2 = Mean Diurnal Range, BIO4 = Temperature seasonality, BIO5 = Max Temperature of the Warmest Month, BIO6 = Min Temperature of the Coldest Month seasonality, BIO12 = Annual Precipitation, BIO13 = Precipitation of the Wettest Month, BIO14 = Precipitation of the Driest Month and BIO15 = Precipitation seasonality.

We conducted a principal component analysis to examine the degree of climatic variation among species, then we ran a MANOVA using informative rotated PC´s, followed by a post-hoc multiple comparison approach using a Bonferroni corrected approach, to evaluate pairwise differences among species. Statistical analyses were performed in software R (R Core Team 2020).

Results

Phylogenetic analysis. The partial cytochrome *b* alignment contained 145 sequences with 1, 140 columns, 620 distinct patterns, 434 informative sites, 66 singleton sites and 640 constant sites. ModelFinder found that the Best-fit model was the Hasegawa-Kishono-Yano, with empirical base frequencies allowing for a proportion of invariable sites plus discrete Gamma model (HKY + F + I + G4), whilst our cytochrome *c* oxidase subunit I alignment contained 61 sequences with 657 columns, 216 distinct patterns, 188 informative sites, 22 singleton sites and 447 constant sites. ModelFinder found Hasegawa-Kishono-Yano, with empirical base frequencies plus discrete Gamma model (HKY + F + G4) as the Best-Fit model according to BIC.

Both maximum likelihood and Bayesian phylogenetic analysis of mitochondrial genes sequences (Figures 1 and 2) from specimens that morphologically match *M. pilosatibialis str. sensu* La Val (1973), were recovered as part of a monophyletic clade containing specimens from Guatemala, El Salvador, and México. This clade was found well-supported in cytochrome *b* analyses, with negligible support found in the cytochrome *c* oxidase subunit I phylogenetic tree. A specimen from Guatemala was geographically closest to the type locality in Honduras, therefore, we followed La Val (1973) in referring to this clade as *M. pilosatibialis str*.

In our cytochrome *b* phylogenetic tree, a clade formed by sequences from specimens of *M pilosatibialis str.* is sister to a well-supported high elevation clade formed by specimens from Chiriquí and Cordillera Oriental (Ecuador), hereafter called *M*. sp. n., whilst our cytochrome *c* oxidase subunit I, analysis retrieved a supported clade from Costa Rica, Panamá and Ecuador samples as sister to *M.* sp. (Quintana Roo, Yucatán, México).

The phylogenetic placement of *M.* sp. (Quintana Roo, Yucatán, México) differs in our cytochrome *b* phylogenetic analysis, being paraphyletic to a well-supported monophy-

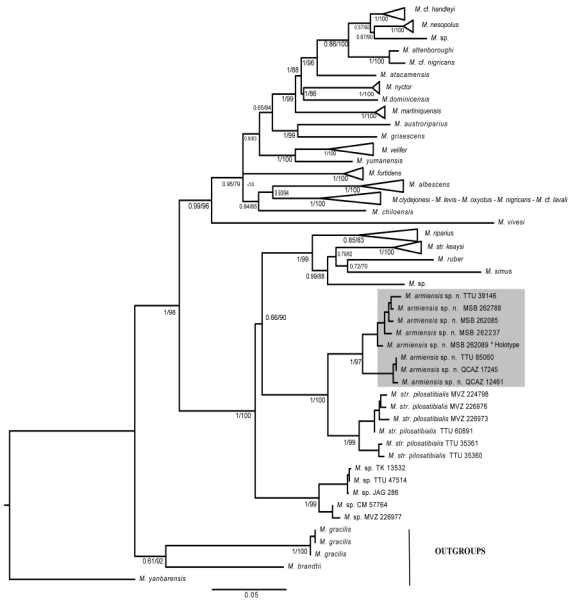

Figure 1. Partial cytochrome *b* phylogeny resulting from bayesian and maximum likelihood inference, with shaded grey sequences of *M. armiensis* sp. n., including holotype. The Bayesian analysis was conducted in MrBayes and maximum likelihood trees were generated using IQ-TREE with 100 bootstraps and 1000 replicates. Scores are bootstrap and probabilities values. Nodal support is shown right and left of slashes (" /") respectively.

letic clade formed by *M.* sp. n. + *M. pilosatibialis str.* and the *ruber* group (*simus, keaysi, ruber, riparius,* sp.). *M*. sp. n. is part of well supported clade in both mitochondrial topologies. Within the *ruber* group, we were able to obtain a cytochrome *b* sequence from a specimen that morphologically matches *M. keaysi sensu* La Val (1973) from Cochabamba, Bolivia which is the specimen geographically nearest to the type locality of Minas at Puno, Perú.

M. sp. n. is genetically distinct using both mitochondrial markers, the genetic pairwise distances between *M*. sp. n. and other species studied range from 6.1 to 12 %, *p*-distance 0.06 – 0.11 in partial cytochrome *b*, and from 3.6 to 9.8 %, *p*-distance 0.03 – 0.08 in partial cytochrome *c* oxidase subunit I. In partial cytochrome *b*, we retrieved the lowest value for conspecific populations

Figure 2. Partial cytochrome oxidase *c* subunit I phylogeny resulting from bayesian inference and maximum likelihood inference. The Bayesian analysis was conducted in MrBayes and maximum likelihood trees were generated using IQ-TREE with 100 bootstraps and 1000 replicates. Scores are bootstrap and probabilities values. Nodal support is shown right and left of slashes (" /") respectively.

from Chiriquí and eastern Cordillera Oriental (Ecuador; 3.1 %, *p*-distance 0.03). For cytochrome oxidase *c* oxidase subunit I, the lowest value was retrieved between conspecific populations from Valle del Silencio (Costa Rica) and Chiriquí Province (Panamá; 0.0 %, p-distance 0.00). Distance values are of the same order of magnitude as other interspecific and intraspecific comparisons within the taxa compared (Table 1).

Our species tree analysis readily identified *M.* sp. n. as genetically distinct from other species in the Neotropical and Nearctic *Myotis* radiation. Although we recovered relatively low support values for the newly identified clade, this topology also depicts a sister species relationship between conspecific populations from Chiriquí (Panamá) and Cordillera Oriental (Ecuador) as previously shown in our mitochondrial phylogenetic analyses (Figure 3). Results from two STACEY replicates analyses using nuclear data set suggested 20 putative species, under two collapse heights (0.0001 and 0.0005). Among the delimitated species, we found *M*. sp. n. as a candidate to be evaluated under an integrative taxonomy approach using independent data.

Morphological analysis. The principal component analysis comparing all five species extracted two major components that accounted for 53.0 and 30.3 % of the variation (Figure 4; Table 2). The PCA plot shows that *M*. sp. n. overlaps partially with *M. pilosatibialis str.*, which is due to size and shape similarities, while all of the other species were distinct. *M. str. keaysi* and *M. oxyotus gardneri* plotted at the lower left end of PC1 reflecting their larger size, whilst *M*. sp.

Table 1. Matrix of genetic distances (partial cytochrome *b* and cytochrome *c* oxidase subunit I) within and among three species of *Myotis*, where *armiensis* sp. n. in divided in two clades in cytochrome *b* analysis and three clades in cytochrome *c* oxidase subunit I. Below the diagonal:pairwise genetic distance using Kimura 2-parameter model (percentage). On the diagonal within clade distance using the Kimura 2-parameter model (percentage). Above the diagonal:pairwise *p*-distance values. Number of specimens sequenced in parenthesis.

	Partial Cytochrome-b				
Species/clades	**1**	**2**	**3**	**4**	**5**
1 *M. armiensis* sp. n. Panamá (5)	**1.0**	0.03	0.06	0.11	0.09
2 *M. armiensis* sp. n. Cordillera Oriental (Ecuador) (3)	3.1	**0.0**	0.06	0.11	0.09
3 *M. pilosatibialis* (6)	6.2	6.1	**2.0**	0.11	0.11
4 *M. keaysi* (1)	12.0	11.7	11.7	**n.a**	0.11
5 *M.* sp. (5)	9.8	10.1	10.0	12.1	**2.0**
	Partial Cyto-chrome c oxidase subunit I				
Species/clades	**1**	**2**	**3**	**4**	**5**
1 *M. armiensis* sp. n. Panamá (2)	0.0	0.01	0.01	0.03	**0.08**
2 *M. armiensis* sp. n. Cordillera Oriental (Ecuador) (1)	1.8	n.a	0.01	0.03	**0.08**
3 *M. armiensis* sp. n. Costa Rica (11)	0.0	1.8	0.0	0.03	**0.08**
4 *M. pilosatibialis* (6)	3.6	3.8	3.6	0.0	**0.07**
5 *M.* sp. (5)	9.5	8.7	9.8	8.1	**1.3**

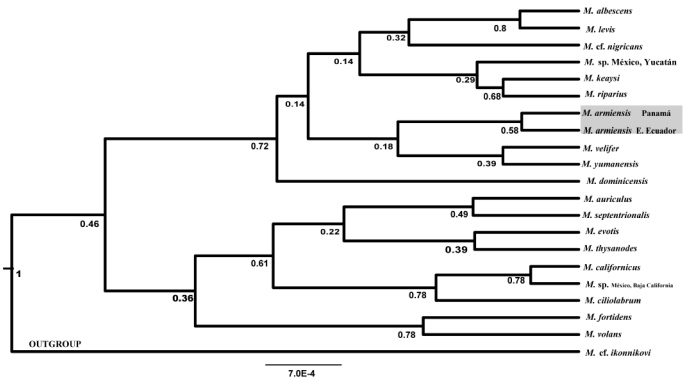

Figure 3. Species tree inferred in *BEAST using multilocus sequence data for New World *Myotis*. Number under branches represent bayesian posterior probability values with conspecific populations from Ecuador and Panama shaded grey.

(Quintana Roo, Yucatán, México) plotted at the right lower end, which is explained by its small size. PC1 shows variation in size and is influenced most by variables related to length of the skull, having MAL, GLS, CCL, CBL, CIL and M1–M3 with loadings above 0.8. PC2 shows shape variation, and it is most influenced by measurements associated with the width of the skull, with BCB and POB having loadings above 0.8.

A one-way multivariate analysis of variance suggested there was a statistically significant difference between all species on both PC1 and PC2, as suggested by Pillai's Trace test, $F_{(8,58)} = 15.411$, $P < 0.001$. Follow-up ANOVAs showed that this dissimilarity occurred at both PC´s (PC1, $F_{(4,29)} = 15.9$, $P < 0.05$, PC2, $F_{(4,29)} = 15.0$, $P < 0.05$). Post-hoc multiple comparison analyses revealed that *M*. sp. n. is different from *M*. *oxyotus gardneri* ($P < 0.01$), and *M*. *str*. *keaysi* ($P < 0.05$)

Table 2. Factor loading after PCA and varimax rotation, with Kaiser Normalization for two principal components from a principal component analysis (PCA). The analysis is based on 15 craniometric measurements of five species, including 33 individuals. See Methods for variable abbreviations.

Measurements	PC I	PC II
MAL	-.939	.231
MAN	-.695	.585
GLS	-.914	.318
CCL	-.862	.444
CBL	-.866	.423
CIL	-.944	.245
BAL	-.754	.574
MAB	-.751	.323
BCB	----	.921
IOB	-.645	.564
POB	-.374	.812
BAC	-.337	.599
BAM	-.513	.761
MTL	-.765	.575
M1-M3	-.840	.299
eigenvalues	11.14	1.34
% of variance explained	53.0	30.3
cumulative %	53.0	83.3

Table 3. Vector coefficient correlations between original variables and discriminant functions (DF1 and DF2) for selected samples of *Myotis*.

Measurements	DF1 (83.5%)	DF2 (9.9%)
MAL	-32.71	-179.89
MAN	135.04	62.82
GLS	215.37	-84.56
CCL	-120.75	-83.33
CBL	42.31	-75.27
CIL	-136.83	-52.95
BAL	70.81	-144.96
MAB	190.98	142.86
BCB	21.57	49.32
IOB	.67	-23.05
POB	18.80	-36.78
BAC	-97.68	106.43
BAM	38.63	-76.04
MTL	-89.95	-23.80
M1-M3	78.38	85.67

in PC1, and different from *M*. sp.(Quintana Roo, Yucatán, México; $P < 0.001$) and *M*. *str*. *pilosatibialis* ($P < 0.05$) in PC2. For other comparison, see Appendix V.

Although *M*. sp. n. is overlapping partially with *M*. *pilosatibialis*, our DFA analysis readily distinguishes *M*. sp. n. from other species along the first axis (83.5 %) and to a lesser extent the second axis (9.9 %, Figure 5; Tabla 3). The jackknifed classification matrix showed that the analysis correctly classified 81.8 % of the specimens, with *M*. sp. n. 70 % correctly classified, *M. str. pilosatibialis* 75 % correctly classified, *M*. sp. (Quintana Roo, Yucatán, México) 100 % correctly classified, *M*. *str. keaysi* 75 % correctly classified, and *M*. *oxyotus gardneri* 100 % classified.

Cranial index of *M*. sp. n. (CRI: 50.6) is larger than *M*. *str. pilosatibialis* (CRI: 47.3), *M*. sp. (Quintana, Roo, Yucatán, México, CRI: 42.1), but smaller than *M*. *str*. *keaysi* (CRI: 51.5) and *M. oxyotus gardneri* (CRI: 53.8).

Climatic analysis. Our PCA for climatic variables resulted in three PCA´s with eigenvalues > 1, explaining 85.6 % of the total variation. PCA1 was primarily informative for Min Temperature of the Coldest Month, whilst Mean Diurnal range was the principal driver along PCA2. In contrast

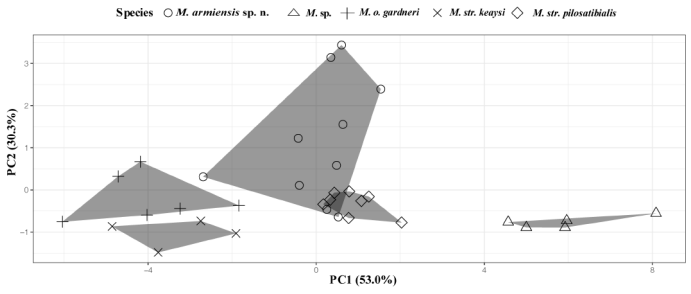

Figure 4. Principal components (PC´s) from a PCA based on 15 cranial measurements from 33 individuals. Samples:*M. armiensis* sp. n (circles), *M.* sp. (triangles), *M. oxyotus gardneri* (+ symbols), *M. keaysi str.* (X symbols), and *M. pilosatibialis str.* (diamonds).

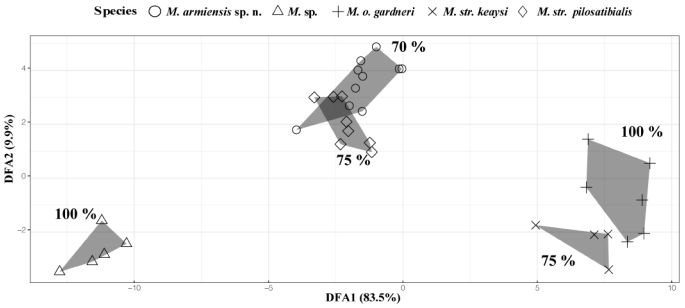

Figure 5. Vector correlation coefficients (loadings) between original variables and discriminant functions (DF1, DF2), with jackknifed percentage of correctly classified specimens for each group. Samples:*M. armiensis* sp. n (circles), *M.* sp (triangles), *M. oxyotus gardneri* (+ symbol), *M. keaysi str.* (x symbol), and *M. pilosatibialis str.*(diamonds).

Annual Temperature was the principal driver of PC3. One-way multivariate analysis of variance suggested there was a statistically significant difference on PC1, PC2, and PC3 as suggested by Pillai's Trace test, $F_{(6, 30)} = 2.283$, $P < 0.1$. Follow-up ANOVAs showed that this dissimilarity occurred at PC3 $F_{(2, 16)} = 4.32$, $P < 0.5$, but not for PC1 $F_{(2, 16)} = 1.50$ ns and PC2 $F_{(2, 16)} = 1.50$ ns. Post-hoc multiple comparison analyses did not reveal statistically significant differences in the climatic envelopes of all species, as indicated by extensive overlap (Figure 6; Table 4).

Discussion

In this report we were able to determine the phylogenetic placement of *M. pilosatibialis str.* based on specimens from Alta Verapaz, Guatemala (San Pedro Carcha, Finca Bethel, 15° 0.61′ N, -90° 0.27′ W), the collecting locality for specimens included in the subspecies description (La Val 1973). This locality is *ca.* 370 km from the type locality at Francisco Morazán, Honduras (14° 0.24 ′N, -85° 0.5′ W), therefore we recommend assigning the name *pilosatibialis* to this species complex, which has a disjunct distribution (primarily low and high elevation species) from southern México, southeastward through Central America into northwestern Panamá, and to the eastern cordillera of the Colombian and Cordillera Oriental (Ecuador). Elsewhere, this complex occurs from the island of Trinidad, to Venezuela and the Colombian Caribbean. This group is characterized by small to medium size, with short woolly hair, and the dorsal surface of tibia partially or entirely covered by fur, which might extend to the hindfoot and across the tibia and onto the plagiopatagium. A flattened occipital region and moderate to high sagittal crest characterize the skull. In agreement with Moratelli *et al.* (2016) and Moratelli *et al.* (2017), we included *pilosatibialis* as part of the *ruber* group based on shared morphological traits (woolly hair, moderate to high sagittal crest, and flat occipital crest) and close molecular evolutionary proximity. Likewise, we determined the phylogenetic placement of *M. keaysi str.*, from voucher specimens collected in Cochabamba, Bolivia (-17° 0.21′S, -65° 0.6′W), located ~600 km distant from the type locality of *M. keaysi* at Inca Mines, Cuzco, Perú (-13° 0.30 ′S ,-70 ° 0.0 W). *Myotis keaysi* is another member of the *ruber* group, with larger external and cranial dimensions, and longer woolly fur, now suggested to be distributed in high elevation sites from the Andes of Colombia, southward to Bolivia and Argentina (Moratelli *et al.* 2013). According to Mantilla-Meluck and Muñoz-Garay (2014) both species are living in sympatry in the Colombian Caribbean and eastern cordillera of the Andes of Colombia.

Larsen *et al.*'s (2012 a, b) molecular study of Neotropical *Myotis* identified an unnamed clade formed by specimens misidentified as *M. nigricans* (TTU 39146 from Santa Clara, Chiriquí, Panamá) and *M. riparius* (TTU 85060 from Azuay, Tungurahua, Ecuador) collected by Robert J. Baker and collaborators in 1983 (Panamá) and 2001 (Sowell-Expedition, Ecuador). Chaverri *et al.* (2016) referred to this clade as *M. keaysi* based on cytochrome *c* oxidase subunit I sequences of unvouchered specimens from Valle del Silencio, Costa Rica and one specimen (ROM 104302), collected by the Royal Ontario Museum in Santa Clara, Ojo de Agua, 2 km N of Santa Clara, Panamá.

Prior to those studies, voucher specimen series of *Myotis* collected from the highlands of Chiriquí Province (USNM, TCWC) had been identified as *M. k. pilosatibialis*. Our bat surveys (in Ecuador in 2017 and Panamá in 2012) provided additional specimens for morphological and genetic studies. Herein, we have examined specimens assigned to the unnamed clade *sensu* Larsen *et al.* (2012 a, b), and found morphometric and genetic differences that support recognition of a new species. We propose that populations from Chiriquí Province (Panamá) and Cordillera Oriental (Ecuador) represent a new species, which is described as follows:

Myotis armiensis, species novum

Armien's Myotis, Myotis de Armién

Figure 7, 8, and 9; Tables 5 and 6

Myotis keaysi pilosatibialis, La Val, 1973, part

Myotis keaysi pilosatibialis, Hernandez-Meza *et al.* 2005, part.

Myotis keaysi pilosatibialis, Wilson, 2008, part.

Myotis nigricans, Larsen *et al*. 2012a, part.

Myotis riparius, Larsen *et al*. 2012b, part.

Myotis keaysi, Chaverri *et al*. 2016, part.

Myotis cf. *pilosatibialis*, Moratelli *et al*. 2016, part.

Myotis cf. *pilosatibialis*, Moratelli *et al*. 2017, part.

Holotype and type locality. Voucher MSB 262089; adult male; preserved as skin, skull and skeleton (Figures 8 and 9) at the Museum of Southwestern Biology (MSB), University of New Mexico collected on 20 March 2012 by Joseph A. Cook and collaborators (Tropical Biology Class 2012 and Instituto Conmemorativo Gorgas de Estudios de la Salud) at La Amistad International Park Ranger Station (8° 89′ N, -82° 61′ W, elevation 2, 214 m), Bugaba District, Chiriquí Province, Panamá. Tissues deposited at the same museum (NK 209314, LN2 preservation), with additional tissues at Instituto Gorgas, Panama City (-80°C preservation). The specimen is well preserved. The measurement for the forearm (44 mm) recorded on the specimen tag is incorrect and should be FA = 39 mm as now recorded in the Arctos Museum Database.

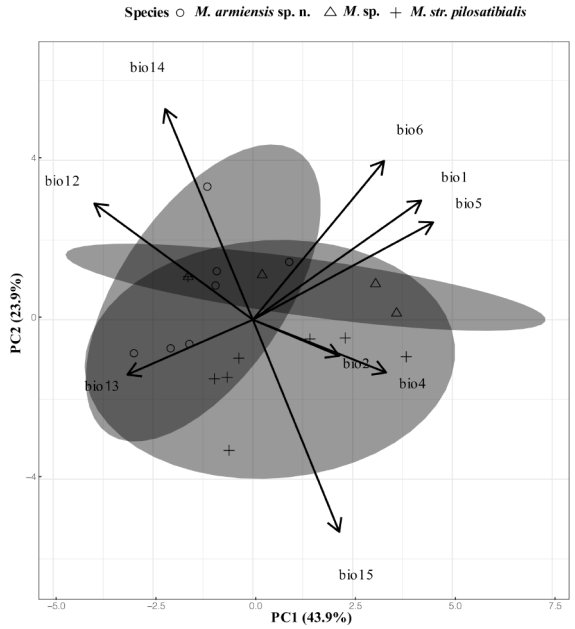

Figure 6. Principal component (PC´s) from a PCA based on 9 bioclimatic variables extracted from 19 distribution localities of *pilosatibialis* species complex, with confidence ellipses and corresponding vectors correlations of climatic variables with the first two eigenvectors. Samples:*M. armiensis* sp. n. (circles), *M.* sp. (triangles), and *M. pilosatibialis str.*(+ symbols).

Paratypes. Nineteen additional specimens were collected from Chiriquí Province, Panamá and Cordillera Oriental (Ecuador). Two specimens were designated as paratypes based on genetic identification, (partial cytochrome *b*), morphometrics and qualitative data: skin of one adult female (MSB 262085), collected by Joseph A. Cook and collaborators, 20 March 2012; skin and skull of one female, adult (TTU 85060) collected by Robert J. Baker and collaborators (Sowell Expedition-Ecuador, 2001), 24 July 2001.

Six paratypes identified solely by genetic identification (partial cytochrome *b*) were collected at Bugaba District,

Table 4. Factor loading after PCA and varimax rotation, with Kaiser Normalization for three principal components from a principal component analysis (PCA). The analysis is based on 9 bioclimatic variables, including 19 localities.

Climatic variable	PC I	PC II	PCIII
Annual Mean Temperature	.972	.209	.086
Mean Diurnal Range	-.013	.697	.027
Temperature Seasonality	.242	.633	.287
Max Temperature of the Warmest Month	.923	.337	.128
Min Temperature of the Coldest Month	.988	-.037	-.036
Annual Precipitation	-.157	-.820	-.480
Precipitation of the Wettest Month	-.241	-.883	.243
Precipitation of the Driest Month	-.048	-.086	-.965
Precipitation Seasonality	.047	.073	.973
eigenvalues	2.9	2.5	2.2
% of variance explained	32.4	27.8	25.3
cumulative %	32.4	60.2	85.6

Figure 7. Adult female of *Myotis armiensis* sp. n. (QCAZ 17245) captured at Cabañas del Aliso, Cosanga, Napo Province, Ecuador. Photographed by Carlos Carrión Bonilla.

Chiriquí Province, Panamá [one adult male (MSB 262237) collected by Joseph A. Cook and collaborators, 20 March 2012)], Jurutungo, Río Sereno, Renacimiento District, Chiriquí Province, Panamá [sex unknown (MSB 262788), collected by Gorgas Institute field researchers, 6 May 2011], Santa Clara, Renacimiento District, Chiriquí Province, Panamá [one female, age unknown (TTU 39146), collected by Robert J. Baker, 19 January 1983], Cabañas del Aliso, Cosanga, Napo Province, Ecuador [one female, age adult, (QCAZ 17245) collected by Carlos A. Carrión Bonilla, 13 December 2017), Yantzaza, Campo Minero Fruta del Norte, Zamora Chinchipe, Ecuador [male, adult (QCAZ 12461), collected by Paula Iturralde, 3 March 2011]. Another specimen from Ojo de Agua, 2 km N of Santa Clara, Renacimiento District, Chiriquí Province, Panamá (ROM 104302), collected by Burton Lim and Eamon O'Toole, on 8 March 1995 was identified based on barcode cytochrome *c* oxidase subunit I.

Ten paratypes identified with morphometric analysis of craniometric measurement analysis and qualitative morphological of skins and skulls were collected from La Amistad International Park Ranger Station, Bugaba District, Chiriquí Province, Panamá [(two females, adults (MSB 262217-18, only skins were studied, no skulls available) collected by Joseph A. Cook and collaborators, 20 March 2012)]; Cerro Punta, Casa Tiley, Tierras Altas District, Chiriquí Province, Panamá [female, adult (USNM 323599, by Handley, C. and Greenwell, F.M., 6 March, 1962)]; El Volcán 2 min S. W, Tierras Altas District, Chiriquí Province, Panamá [two females, adults, (USNM 331942, USNM 331943, by Tyson E, collected 21 March 1962)]; Cuesta de Piedra, Tierras Altas District Chiriquí Province, Panamá [female, adult (USNM 331953, by Tyson E, 28 March 1962)]; 36 km, north of Concepción, Bugaba District, Chiriquí Province, Panamá [five females, adults (TCWC 12655-59, by Patten, D.R., 8 June 1964)]. We did not include any specimens from Costa Rica in the type series, because the Chaverri *et al*. (2016) study was unvouchered, and therefore morphological confirma-

Table 6. Selected measurements, cranial index, body mass (adults males and females[*N*]). Mean, (Minimum–Maxima) and sample size (*n*). See methods for variable abbreviations.

Characters	*M. armiensis sp. n.* Chiriquí (Panamá) and Cordillera Oriental (Ecuador)	*M. keaysi str.* Perú	*M. pilosatibialis str.* El Salvador Honduras México	*M. sp.* Quintana Roo, Yucatán, México	*M. oxyotus gardneri* Costa Rica and Panamá
Body mass	5.0 (4.5–5.6) *n* = 10	6.0 *n* = 1	6.1 *n* = 1		8 *n* = 1
HB	86 (77–92) *n* = 12	94.0 *n* = 1			93.0 (87–98) *n* = 3
Tail	39 (32–48) *n* = 13	42.0 *n* = 1			40.3 (39–43) *n* = 3
Foot	8 (7–10) *n* = 13	8.0 *n* = 1			8.3 (8–9) *n* = 3
Ear	13 (11–14) *n* = 13	14.0 *n* = 1			15.7 (15–16) *n* = 3
LDF	6.2 (5.3–7.4) *n* = 10				7.7 (7.4–7.9) *n* = 3
LVF	6.3 (4.5–8.3) *n* = 10				6.6 (5.6–7.2) *n* = 3
FA	38.0 (36.3–39.4) *n* = 13	40.2 *n* = 1	35.9 (34.3–37.1) *n* = 5	32.6 (31.8–34.4) *n* = 4	40.4 (38.0–42.8) *n* = 6
3MC	34.3 (32.9–35.9) *n* = 13	36.8 *n* = 1	33.2 (32.1–34.4) *n* = 5	29.3 (27.7–30.4) *n* = 4	36.3 (34.5–38.6) *n* = 6
GLS	13.5 (13.0–14.0) *n* = 10	14.5 (14.1–15.0) *n* = 5	13.6 (13.5–13.9) *n* = 8	12.7 (12.6–13.0) *n* = 4	14.5 (14.1–15.0) *n* = 6
CCL	12.1 (11.7–12.5) *n* = 10	12.6 (12.0–13.0) *n*= 5	12.1 (11.8–12.3) *n* = 8	11.4 (11.2–11.7) *n* = 4	12.8 (12.3–13.3) *n* = 6
CBL	12.7 (12.3–13.0) *n* = 10	13.3 (12.6–13.8) *n* = 5	12.7 (12.4–12.9) *n* = 8	12.1 (11.7–12.4) *n* = 4	13.5 (13.1–14.1) *n* = 6
CIL	12.7 (11.9–13.2) *n* = 10	13.5 (12.9 –14.0) *n* = 5	12.9 (12.7–13.1) *n* = 8	12.1 (11.8–12.5) *n* = 4	13.7 (13.2–14.2) *n* = 6
BAL	11.7 (11.3–12.1) *n* = 10	12.1 (11.5–12.5) n = 5	11.6 (11.3–11.9) *n* = 8	11.0 (10.7–11.3) *n* = 4	12.4 (12.0–12.8) *n* = 6
ZB	8.5 (7.9–8.8) *n* = 8	8.6 (8.5–8.8) *n* = 4	8.2 (8.1–8.4) *n* = 6		8.9 *n* = 1
MAB	7.0 (6.6–7.4) *n* = 10	7.0 (6.9–7.2) *n* = 5	7.0 (6.9–7.2) *n* =8	6.7 (6.6–6.7) *n* = 4	7.3 (7.1–7.4) *n* = 6
BCB	6.8 (6.2–7.3) *n* = 10	6.5 (6.4 –6.5) *n* = 5	6.3 (6.1–6.5) *n* =8	5.9 (5.8–6.0) *n* = 4	6.8 (6.6–7.0) *n* = 6
IOB	4.5 (4.2–4.8) *n* = 10	4.7 (4.5–4.9) *n* =5	4.3 (4.2–4.5) *n* = 8	4.0 (3.9–4.1) *n* = 4	4.7 (4.5–4.9) *n* = 6
POB	3.6 (3.2–4.2) *n* = 10	3.6 (3.4–3.8) *n* = 4	3.4 (3.3–3.5) *n* = 8	3.1(3.1–3.2) *n* = 4	3.9 (3.8–4-0) *n* = 6
BAC	3.6 (3.4–4.0) *n* = 10	3.6 (3.5–3.7) *n* = 5	3.6 (3.5–3.8) *n* = 8	3.3 (3.2–3.4) *n* = 4	3.6 (3.4–3.8) *n* = 6
BAM	5.5 (5.3–6.0) *n* = 10	5.6 (5.4–5.8) *n* = 5	5.3 (5.2–5.5) *n* = 8	4.9 (4.7–5.0) *n* = 4	5.7 (5.5–5.8) *n* = 6
MTL	5.2(5.1–5.4) *n* = 10	5.5 (5.2–5.6) *n* = 5	5.1(5.0–5.2) *n* = 8	4.8(4.6–4.9) *n* = 4	5.5 (5.4–5.6) *n* = 6
M1–3	2.9 (2.5–3.0) *n* = 10	3.1 (3.0–3.3) *n* =5	2.9 (2.8–3.0) *n* = 8	2.6 (2.5–2.6) *n* = 4	3.1 (3.1–3.2) *n* = 6
MAL	9.6 (8.9–10.3) *n* = 10	10.2 (9.9–10.5) *n* =5	9.6 (9.5–9.7) *n* = 8	9.1 (8.8–9.3) *n* = 4	10.4 (10.0–10.9) *n* = 6
MAN	5.5 (5.3–5.7) *n* = 10	5.8 (5.6–5.9) *n* = 5	5.5 (5.4–5.7) *n* =8	5.1 (4.9–5.2) *n* = 4	5.7 (5.7–5.9) *n* = 6
CRI	50.6 (47.0–53.7) *n* = 10	51.5 (49.7–53.9) *n* = 5	47.3 (45.8–49.1) *n* = 8	42.1 (41.1–43.3) *n* = 4	53.8 (50.7–56.0) *n* = 6
MAX	18.1 (17.2–19.6) *n* = 10	18.8 (17.6–19.9) *n* = 5	17.3 (16.7–17.9) *n* = 8	15.0 (14.0–15.5) *n* = 4	19.2 (18.4–19.8) *n* = 6

tion is not possible.

Distribution. *Myotis armiensis* sp. n. is known from the premontane and montane forest of Chiriquí Province, Panamá, extending its distribution into La Amistad International Park in Panamá (Las Nubes Rangers Station) and Costa Rica (Valle del Silencio). Elevation in Panamá and Costa Rica varies from 975 m to 2,500 m: Concepción (≈ 8°.51′ N, -82°.62′ W, 2,011m), Cerro Punta (8°.88′ N, -82°.73′ W, 1,280 m), Cuesta de la Piedra (8°.88′ N, -82°.73′ W, 975 m), El Volcán (8°.88′ N, -82°.73′W, 1,280 m), Parque Internacional la Amistad Ranger Station: (8°.89′ N, -82°.61 W, 2, 214 m), Jurutungo, Río Sereno (8°.9′ N, -82°.73 W, 2,219 m),

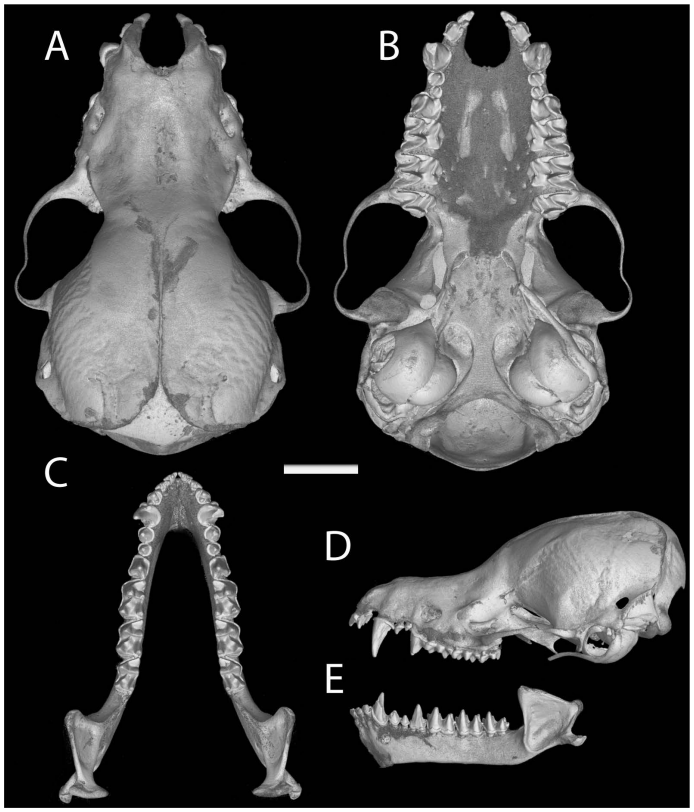

Figure 8. Dorsal (A) and ventral view (B) of the cranium, dorsal view of the mandible (C), and lateral view of the cranium (D) and mandible of the holotype of *M. armiensis* sp. n. (MSB 262089). Scale bar = 5 mm. Photograph taken by John Korbin (Sandia National Laboratory-New Mexico, USA).

Santa Clara (≈ 8°.83′N, -82°.75′W, ≈ 1,178 m), Ojo de Agua, Santa Clara (8° 42′ N, -82°.45 W, 1,500 m), Valle del Silencio, Costa Rica (9° 11′ N, -82°.96 W, 2,500 m). In Ecuador, *M. armiensis* sp. n. is known from Cordillera Oriental. Elevation in Ecuador varies from 1,200 m to 2,249 m: Yantzaza, Campo Minero Fruta del Norte, Zamora Chinchipe (-3°.75′S, -78°.53′W, 1, 200 m), Colonia Azuay, Tungurahua Province, Ecuador (-1°.34′ S, -78.20°, 1,660 m), Cabañas el Aliso, Sector Las Caucheras, Quijos, Napo Province (-3°.75′ S, -78°.53′ W, 2,249 m). See Figure 10 for species distribution in Costa Rica, Panamá and Ecuador.

Etimology. *Myotis armiensis* honors Dr. Blas Armién in recognition of his outstanding contributions to research in zoonotic emergent diseases, public health, and mammalogy in Panamá. Over two decades, he has supported the systematic development of holistic museum collections, including associated cryogenic biorepositories and parasites. This infrastructure (>11,000 specimens) is now the basis for new insights into temporal and spatial aspects of the biology of Panama's mammals and associated parasites and pathogens.

Diagnosis. Due to the dearth of availability of substantial specimen material and despite the lack of a single morphological character that consistently distinguishes *M. armiensis* from the rest of Neotropical congeners, *Myotis armiensis* can be distinguished by a combination of the following morphological traits: pelage is short and woolly, dorsal and ventral fur bicolored; insertion of the plagiopatagium occurs on the foot at the level of the base of toes by a wide membrane; lack or relatively low presence of fur on dorsal surface of tibia, foot and plagiopatagium, and border of the uropatagium without a fringe; skull is moderately large; forehead is steeply sloping; rostrum is long; lambdoidal crest is present and high; sagittal crest present, with height from low to medium; occipital crest is absent; occipital region flattened and the shape of the braincase is globular.

Table 5. Selected measurements (mm) and body weight (g) of the holotype (MSB 262089) and paratype material of *Myotis armiensis*. See methods for variable abbreviations.

Characters	MSB 262089 ♂	Paratypes
Body mass	5	5 (4.5–5.6) *n* = 9
HB	90	85 (77–92) *n* = 11
Tail	38	39 (32–48) *n* = 12
Foot	8	8 (7–10) *n* = 12
Ear	13	14 (11–14) *n* = 12
LDF	6.4	6.1 (5.3–7.4) *n* = 9
LVF	7.2	6.2 (4.5–7.4) *n* = 9
FA	37.1	38.1 (36.3–39.4) *n* = 12
3MC	34	34.3 (32.9–35.9) *n* = 12
GLS	13.3	13.5 (13.0–14.0) *n* = 9
CCL	12.2	12.1 (11.7–12.5) *n* = 9
CBL	12.3	12.8 (12.5–13.0) *n* = 9
CIL	11.9	12.8 (12.2–13.2) *n* = 9
BAL	12.1	11.6 (11.3–11.9) *n* = 9
ZB	7.9	8.6 (8.0–8.8) *n* = 7
MAB	6.6	7.1 (6.6–7.4) *n* = 9
BCB	7.3	6.8 (6.2–7.2) *n* = 9
IOB	4.4	4.6 (4.2–4.8) *n* = 9
POB	4.2	3.5 (3.2–3.7) *n* = 9
BAC	3.6	3.7 (3.4–4.0) *n* = 9
BAM	5.4	5.6 (5.3–6.0) *n* = 9
MTL	5.2	5.2 (5.0–5.4) *n* = 9
M1–3	2.7	2.9 (2.5–3.0) *n* = 9
MAL	9.5	9.6 (8.9–10.3) *n* = 9
MAN	5.7	5.5 (5.3–5.7) *n* = 9

Myotis armiensis can be readily distinguished from *Myotis* congeners from Central and South America based on gene trees [partial sequence of cytochrome-*b* (~710 pb) and partial cytochrome *c* oxidase subunit I (~ 657 pb)] and species tree phylogenetic analysis of one exon: recombination activating gene II (RAG2), and 3 intron regions: protein kinase C, iota (PRKCI), signal transducer and activator of transcription 5A (STAT5A), and thyrotropin (THY). Finally, molecular synapomorphies in mitochondrial and intron genes regions sequences support the species level recognition of *M. armiensis* sp. n. compared to other species in the New World *Myotis* radiation (Appendix VI– X). These served as diagnostic characters for the species.

Description. A medium to large species of *Myotis* (FA 36.3–39.4 mm, *n* = 13 and weight 4.5-5.6 gr, *n* = 10); other

Figure 9. Dorsal and ventral views of the skins of the holotype of *M. armiensis* sp. n. (MSB 262089), *M. pilosatibialis str.*(TCWC 24101, paratype), and *M. keaysi str.* (MSB 70381). Scale bar = 10 mm.

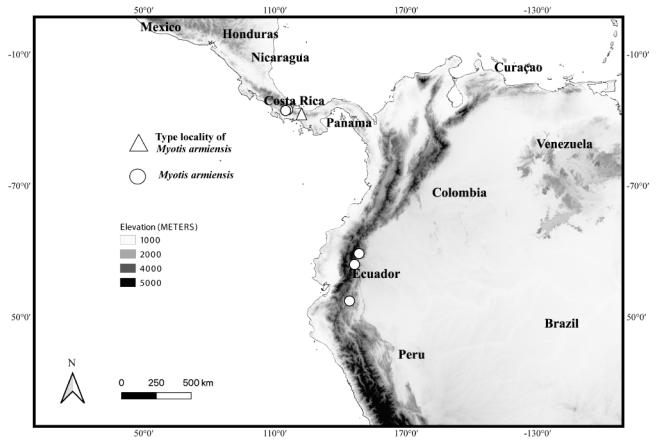

Figure 10. Map of part of Central and South America showing localities examined for *M. armiensis*, with triangle (type locality) and distribution in Costa Rica, Panamá, and Ecuador with circles. See Appendix I for localities of examined in Panamá and Ecuador.

measurements (Tables 5 and 6), with external size larger than *M. pilosatibialis str.*, *M.* sp. (Quintana Roo, México) and smaller than *M. oxyotus gardneri*, and *M. keaysi str*. Ears are brown in color, comparatively small to medium-sized (EL 11–14 mm). Dorsal and ventral fur is woolly and short (LDF 5.3 -7.4 mm, LVH 4.5-8.3 mm). Dorsal pelage is bicolor, with brown to dark brown at the base and from brown to Mummy Brown at the tips. Ventral pelage is bicolor, with Buckthorn Brown to buff at the tips and dark brown to black at the base. Abdomen is bicolor, from Buckthorn Brown to black with buff tips. Sides and wing color are dark brown or Cinnamon Brown to Mummy Brown. Uropatagium and plagiopatagium are Mummy Brown or Cinnamon Brown. Insertion of the plagiopatagium occurs at the foot at the level of the base of toes by a wide membrane. The uropatagium lacks fringing hairs along the trailing edge. Fur presence on tibia, foot and plagiopatagium, with fur extending across a quarter or less than this at the base of the dorsal and ventral side of uropatagium. Skull and mandible are medium-size (GLS 13.0 –14.0 mm, MAL 8.3–10.3). The dental formula is: 2/3, 1/1, 3/3, 3/3 = 38. In the holotype, the second upper premolar (p3) is aligned and visible in lateral view. Rostrum is long and frontals are steeply sloping; lambdoidal crest is well developed and occipital region is flattened.

Comparisons. In comparison with species in the *ruber* group, *M. armiensis* sp. n. differs from *simus* and *riparius* by having a less contrasting dorsal and ventral coloration (dorsal fur with dark brown to Mummy Brown and ventral fur with Buckthorn Brown to dark brown), with more contrasting (Orange-Brown or Chocolate) in *simus*, (golden -yellow) in *midastactus*, (ventral hairs with dark brown based and yellowish tips/reddish-brown or cinnamon brown dorsal color) in *riparius*, (Bister Brown color of dorsal hairs at tips and buff to orange of ventral color at tips) in *pilosatibialis* [type material]. *M. armiensis* sp. n. can be distinguished from *keaysi* by having shorter woolly hair on dorsal and ventral side, with longer woolly hair, larger proportion of fur on dorsal and ventral side of the uropatagium, and furrier tibia in *keaysi*. It differs from *simus* by having the plagiopatagium attached broadly to the side of the foot at the level of the toes; with a narrow band of membrane (< 1.5 mm) attached to foot or ankles and with extremely short and woolly fur in *simus*. *M. armiensis* sp. n. shares the flattened occipital region and a moderate to high sagittal crest with members of the *ruber* group. It can be distinguished from *M. ruber* by presence of woolly hair, with silky pelage in *ruber*. Cranial index of *M. armiensis* sp. n. is only larger that *M. pilosatibialis str.* but smaller than other congeners in the *ruber group* (CRI: *armiensis* = 47.0–53.7 , *pilosatibialis* = 45.8–49.1, *keaysi* = 49.7–53.9; *simus* = 73.0–88.1; *ruber* = 78.4–85.0; *riparius* = 64.6–76.1), reflecting a narrower skull configuration.

Myotis armiensis sp. n. differs from the *albescens* group (*albescens*, *handleyi*, *nesopolus*, *nigricans*, *oxyotus oxyotus*, *oxyotus gardneri*, *izecksohni*, *lavali* and *levis*) by having short woolly hair. It only shares the woolly hair trait with *chiloensis*. In addition, it can be distinguished from *albescens* group by the presence of a moderate sagittal crest [absent in *albescens*, very low or absent in *oxyotus*, absent in *nigricans* or very low, absent in *lavali*, very low in *chiloensis*]. *Myotis armiensis* sp. n. differs from *levis* and *albescens* by the absence of fringe of hairs along the edge of the uropatagium. Occipital region is flattened in *M. armiensis* sp. n. [rounded in *albescens*, *oxyotus*, *lavali*, *nigricans*]. The cranial index for *albescens* group is larger than *M. armiensis* sp. n, having the narrowest skull configuration in comparison with this species group.

Reproductive data. One pregnant female with one embryo (MSB 262085) collected by Joseph A. Cook and collaborators at Las Nubes Ranger Station, La Amistad International Park, 20 March 2012. Another female (USNM 323599) with embryo (crown-rump = 3 mm) collected at Cerro

Punta, Casa Tiley, Chiriquí Province, collected by Greenwell, F. M, 6 March 1962. In Ecuador, one pregnant female (TTU 85060) with embryo (crown-rump = 3 mm) collected by Robert J. Baker and collaborators (Sowell-Expedition, 2001) at Colonia Azuay, Tungurahua Province, 24 July, 2001.

Habitat and ecological notes. Las Nubes Ranger Station, the type locality for this new species, is part of a natural corridor (401, 000 ha) of relatively undisturbed montane habitats of the eastern Talamanca Mountains that rise between the Pacific and Caribbean coastlines of Panamá and Costa Rica (Morrone 2017). At La Amistad International Park, Las Nubes Ranger Station, *M. armiensis* sp. n. was found to occur sympatrically with *Desmodus rotundus*, *Anoura geoffroyi*, *Sturnira* cf. *burtonlimi*, *Sturnira mordax*, *Enchistenes hartii* (Phyllostomidae), and *Tadarida brasiliensis* (Molossidae). All captures in 2011, 2012 were with ground mist nets located on the edge of secondary growth forest near Las Nubes Rangers Station. Specimens were collected at a clearing on the edge of the forest (Cerro Punta, Casa Tiley) and in montane forest near a lake shore and moist montane secondary growth forest (2 miles S. W of El Volcán). We did not record any other species of *Myotis* living in sympatry at La Amistad International Park, but based on historic samples, the nominal subspecies *M. oxyotus gardneri* was found in sympatry with the new species at Cerro Punta and El Volcán.

At Valle del Silencio Costa Rica, *M. armiensis* sp. n. was found with *Sturnira burtonlimi*, *Dermanura tolteca*, *Hylonycteris underwoodi*, *Anoura cultrata* (Phyllostomidae), and *Lasiurus blossevillii, Myotis* cf. *nigricans*, and *M. oxyotus gardneri* (Vespertilionidae). The vegetation there was characterized by the presence of oak trees (*Quercus* spp) and bamboo (*Chusquea spp*.), although some sites at Valle del Silencio were dominated by swampy bogs (Chaverri *et al.* 2016).

In Ecuador, *M. armiensis* sp. n. is known from premontane and montane cloud forest of Cordillera Oriental. These forests correspond to Evergreen Lower Montane Forest and Cloud Montane Forest (Bosque Siempreverde Montano Bajo and Bosque de Neblina Montano; Valencia *et al.* 1999). One specimen of *M. armiensis* sp. n. was netted across a trail leading to secondary growth forest in Cabañas del Aliso, Cosanga, Quijos Valle, Napo Province in December, 2017. Other species captured in sympatry at that location were: *Sturnira bogotensis*, *Carollia brevicauda* (Phyllostomidae), *Tadarida brasiliensis* (Molossidae), and *M. oxyotus oxyotus* and *Histiotus montanus* (Vespertilionidae). The vegetation there was characterized by the presence of epiphytes (moss, ferns, orchids, bromeliads) , bamboo (*Chusquea spp.*), and pepper plants (*Piper spp*. and *Peperomia spp.*). Another specimen of *M. armiensis* sp. n. was captured in Colonia Azuay, Tungurahua Province at the north side of the Río Pastaza. This locality is bisected by the Río Topo, a tributary of the Pastaza river and comprises secondary forest and fruit orchards (Haynie *et al.* 2006). Other bat species captured in sympatry at that location were: *Anoura caudifer*, *Artibeus lituratus*, *Carollia perspicillata*, and *Sturnira erythromus*. (Phyllostomidae).

Remarks. It was not possible to examine a set of fluid preserved specimens (*n* = 43) collected at La Amistad International Park Ranger Station, Bugaba District, Chiriquí Province, collected in 2018 by Joseph A. Cook and collaborators (Tropical Biology Class 2018 and Gorgas Institute field workers). Those specimens, until recently housed at the Gorgas Institute in Panama, may represent *M. armiensis* sp. n., but confirmation will require further molecular and morphological analysis (MSB 262086 –88, MSB 262219–262224, 268090–93, MSB 327505–327516, MSB 327520, MSB 327522 –327527, MSB 327575–578, MSB 327601–602, MSB 327649–50, MSB 327700, MSB 327703, MSB 327705, MSB 327709, MSB 327712, MSB 327956).

Based on this report and other museum collections records, the diversity of *Myotis* comprises at least six species in Panamá: *M. albescens*, *M. oxyotus gardneri*, *M. riparius*, *M. pilosatibialis*, *M. nigricans s.l.*, and *M. armiensis* sp. n. In Ecuador, the recognition of this newly identified lineage, increases the diversity to eight species of *Myotis*: *M. albescens*, *M. riparius*, *M. simus*, *M. oxyotus oxyotus*, *M. diminutus*, *M. keaysi*, *M. nigricans s.l.*, and *M. armiensis* sp. n. In Costa Rica, *Myotis* diversity increases to seven species: *M. elegans*, *M. riparius*, *M. albescens*, *M. pilosatibialis*, *M. nigricans s.l.*, *M. oxyotus. gardneri* and now *M. armiensis* sp. n.

Nomenclatural statement.— A life science identifier (LSID) number was obtained for new species described herein: urn:lsid:zoobank.org:pub:9EB39E62-C9AC-41C0-AE76-9C5325608BEE.

Conservation. Myotis armiensis sp. n. is restricted to higher and cooler mountain forest of Panamá, Costa Rica and Cordillera Oriental (Ecuador). These habitats are susceptible to the effects of climate change, in addition to ongoing habitat destruction. This report aims to contribute to efforts to study these environments and more narrowly add to our understanding of species limits of this elusive group of bats.

Acknowledgments

We would like to honor S. Anderson for demonstrating throughout his life of fieldwork in mammalogy (extending from Janos, Chihuahua to Tarija, Bolivia) the immense, multifaceted, and lasting value of each voucher specimen to science and society. Likewise, we especially like to thank R. Moratelli for providing access to morphological and morphometric data from Central America and South American *Myotis*. The completion of this research would have not been possible without his generous offer of this information. We would like to thank also P. A Menendez (McGill University, Canada) for his help with statistical analyses. The following curators and collection managers provided access to specimens under their care: S. Burneo, A. Camacho (Museo de Zoología QCAZ-Pontificia Universidad Católica del Ecuador, Quito-Ecuador); B. Patterson (Field Museum of Natural History, Chicago); E. Lacey, J. Patton, C. Conroy (Museum of Vertebrate Zoology, Berkeley); J. Dunnum and M. Campbell (Museum of Southwestern

Biology, Albuquerque); R. Bradley, C. D. Philips, and H. Garner (Museum of Texas Tech University, Lubbock); J. K. Braun and B. S. Coyner (Sam Noble Oklahoma Museum of Natural History, Norman); K. Bell (Natural History Museum of Los Angeles County); D. Lunde and A. Gardner (Smithsonian National Museum of Natural History, Washington, D.C.); and J. Light (Biodiversity Research and Teaching Collections, College Station). Although not accessible to the first author, previously, N. Simmons and E. Westwig (American Museum of Natural History) provided specimen access to R. Moratelli and he kindly shared those data. We thank J. Korbin of Sandia National Laboratory for graciously preparing and providing the CT Scans of the skull of the holotype specimen. Support for C. A. Carrión Bonilla was from the Instituto de Fomento al Talento Humano IFTH -Ecuador. Laboratory work in Ecuador was funded by the Secretary de Educación Superior, Ciencia, Tecnología e Innovación del Ecuador SENESCYT (Arca de Noé Initiative, O. Torres and S. Ron, Principal Investigators), and grants from Pontificia Universidad Católica del Ecuador. Field work in Ecuador and Panamá was supported by Latin American Institute's Field Research Grant program at the University of New Mexico and Museum of Southwestern Biology. We would like to thank the personnel of the Gorgas Institute, Panama and the many scientists that collected and preserved specimens of *Myotis* over many years or that submitted DNA sequences *Myotis* to GenBank, making them accessible to this study.

Literature cited

Baud, F. J., and H. Menu. 1993. Paraguayan bats of the genus *Myotis*, with a redefinition of *Myotis simus* (Thomas, 1901). Revue Suisse de Zoologie 100:595-607.

Baird, A. B., D. M. Hillis, J. C. Patton, and J. W. Bickham. 2008. Evolutionary history of the genus *Rhogeessa* (Chiroptera: Vespertilionidae) as revealed by mitochondrial DNA sequences. Journal of Mammalogy 89:744-754.

Beck, M. W. 2017. ggord: Ordination Plots with ggplot2. R Package version 1.0.0.

Bouckaert, R., T. G.Vaughan, J. Barido-Sottani, S. Duchêne, M. Fourment, A. Gavryushkina, J. Heled, G. Jones, D. Kühnert, N. De Maio, M. Matschiner, F. K Mendes, N. F. Müller, H. A, Ogilvie, l. Du Plessis, A. Popinga, A. Rambau, D. Rasmussen, I. Siveroni, M. A. SucharD, C-H. Wu, D. Xie, C. Zhang, T. Stadler, and A. J. Drummonds. 2019. BEAST 2.5: An advanced software platform for Bayesian evolutionary analysis. Plos Computational Biology 15:1-28.

Bickford, D., D. J. Lohman, Navjot. S. S, P. K. L, Ng , R. Meier, K. Winker, K. K. Ingram, and I. Das. 2007. Cryptic species as a window on diversity and conservation. Trends in Ecology & Evolution 22:148-155.

Carøe, C., S. Gopalakrishnan, L. Vinner, S. S. T. Mak, M. H. S. Sinding, J. A. Samaniego, N. Wales, T. Sicheritz-Ponten, and M. T. P. Gilbert. 2018. Single-tube library preparation for degraded DNA, Methods in Ecology and Evolution 9:410-419.

Chaverri, G., I. Garin, A. Alberdi, L. Jimenez, C. Castillo-Salazar, and J. Aihartza. 2016. Unveiling the hidden bat diversity of a neotropical montane forest. Plos one, 11:e0162712.

Clare, E. L., B. K. Lim, M. B. Fenton, and P. D. N. Hebert. 2011. Neotropical Bats: Estimating Species Diversity with DNA Barcodes. Plos One 6:1-14.

De Queiroz, K. 2007. Species Concepts and Species Delimitation. Systematic Biology 56:879 - 886.

Dierckxsens, N., P. Mardulyn, and G. Smits. 2016. NOVOPlasty: de novo assembly of organelle genomes from whole genome data. Nucleic Acids Research 45:1-9.

Dunnum, J. L., B. S, McLean, R. C. Dowler, and The Systematic Collections Committee of the American Society of Mammalogist. 2018. Mammal collections of the Western Hemisphere: a survey and directory of collections. Journal of Mammalogy 99:1307-1322.

Edgar, R. C. 2004. MUSCLE: multiple sequence alignment with high accuracy and high throughput. Nucleic Acids Research 32:1792-1797.

Eick, G. N., D. S. Jacobs, and C. A. Matthee. 2005. A nuclear DNA phylogenetic perspective on the evolution of echolocation and historical biogeography of extant bats (Chiroptera). Molecular Biology and Evolution 22:1869-1886.

Fick, S. E., and R. J, Hijmans. 2017. WorldClim2: new 1km spatial resolution climate surface for global land areas. International Journal of Climatology 37:4302-4315.

Florio, A. M., C. M. Ingram, H. A. Rakotondranovy, E. E. Louis, C. J. Raxworthy. 2012. Detecting cryptic speciation in the widespread and morphologically conservative carpet chamelon (*Furcifer lateralis*) of Madagascar. Journal of Evolutionary Biology 25:1399-1414.

Flot, J. F. 2010. SEQPHASE: a web tool for interconverting phase input/output files and fasta sequence alignments. Molecular Ecology Resources 10:162-166.

Fox, J., and S. Weisberg. 2019. An R Companion to Applied Regression. Third edition. Sage, Thousands Oaks CA.

Galbreath, K. E., E. P. Hoberg, J. A. Cook, B. Armién, K. C. Bell, M. L. Campbell, J. Dunnum, A. T. Dursahinhan, R. P. Eckerlin, S. L. Gardner, S. E. Greiman, H. Henttonen, F. A. Jiménez, A. VA. Koehler, B. Nyamsuren, V. V. Tkach, F.Torres-Pérez, A.Tsvetkova ,and A. Hope. 2019. Building an integrated infrastructure for exploring biodiversity: field collections and archives of mammals and parasites. Journal of Mammalogy 100:382-393.

Haynie, M. L., J. G. Brant, L. R. McAliley, J. P. Carrera, M. A, Revelez, D. A, Parish, X. Viteri, C. Jones, and C. J. Phillips. 2006. Investigations in a Natural Corridor between two national parks in Central Ecuador: Results from the Sowell Expedition, 2001. Occasional Papers, Museum of Texas Tech University 263:1-16.

Heled, J., and A. J. Drummond. 2010. Bayesian Inference of Species Trees from Multilocus Data. Molecular Biology and Evolution 27:570-580.

Hernandez-Meza, B., Y. Dominguez-Castellanos, and J. Ortega. 2005. *Myotis keaysi*. Mammalian Species 785:1-3.

Hoffmann, F. G., and R. J. Baker. 2001. Systematics of bats of the genus *Glossophaga* (Chiroptera: Phyllostomidae) and phylogeography in *G. soricina* based on the cytochrome-b gene. Journal of Mammalogy 82:1092-1101.

Honaker, J., G. King, and M. Blackwell. 2011. Amelia II: A Program for Missing Data. Journal of Statistical Software 45:1-47.

Jones, G. 2017. Algorithmic improvements to species delimitation and phylogeny estimation under the multispecies coalescent. Journal of Mathematica Biology 74:447–467.

Jones, G. speciesDA.jar. htpp://indriid.com/2014/speciesDA.jar. Accessed 15 July 2020.

Kalyaanamoorthy, S., B. Q. Minh, T. K. F. Wong, A. von Haeseler, and L. S. Jermiin. 2017. ModelFinder: fast model selection for accurate phylogenetic estimates. Nature Methods 14:587-591.

Kassambara, A. 2020. Rstatix: Pipe-Friendly Framework for Basic Statistical Test. R package version 0.6.0.

Kassambara, A., and F. Mundt. 2020. factoextra: Extract and Visualize the Results of Multivariate Data Analyses. R package version 1.0.7.999.

Kawai, K., N. Kondo, N. Sasaki, D. Fukui, H. Dewa, M. Sato, and Y.yamagai. 2006. Distinguishing between cryptic species *Myotis ikonnikovi* and *M. brandtii gracilis* in Hokkaido, Japan: Evaluation of a novel diagnostic morphological feature using molecular methods. Acta Chiropterologica 8:95-102.

Kawai, K., M. Nikaido, Harada, S. Matsumura, L-K, Lin, Y.Wu, M. Hasegawa, and N. Okada. 2003. The status of the Japanese and East Asian bats of the genus *Myotis* (Vespertillonidae) based on mitochondrial sequences. Molecular Phylogenetics and Evolution 28:297-307.

Koopman, K. F. 1983. Two general problems involved in systematics and zoogeography of bats. Pp. 412-415 in Advances in herpetology and evolutionary biology. Essays in honor of Ernest E Williams (Rhodin, G. J., and K. Miyata, eds). Museum of Comparative Zoology, Cambridge, Massachusetts, EE.UU.

Kumar, S., G. Stecher, and K. Tamura. 2016. MEGA7: Molecular Evolutionary Genetics Analysis Version 7.0 for Bigger Datasets. Molecular Biology and Evolution 33:1870-1874.

La Val, R. K. 1973. A revision of Neotropical bats of the genus *Myotis*. Natural History Museum of Los Angeles County. Science Bulletin:1-54.

Lack, J. B., Z. P. Roehrs, C. E. Stanley, M. Ruedi, and R. A. Van den Bussche. 2010. Molecular phylogenetics of *Myotis* indicate familial-level divergence for the genus Cistugo (Chiroptera). Journal of Mammalogy 91:976-992.

Larsen, R. J., M. C. Knapp, H. H. Genoways, F. A Anwarali Khan, P. Larsen, D.Wilson, and R. J. Baker. 2012a. Genetic Diversity of Neotropical Myotis (Chiroptera: Vespertilionidae) with an Emphasis on South American Species. Plos One 7:1-9.

Larsen, R. J., P. Larsen, H. H. Genoways, F. M. Catzeflis, K. Gelusos, G.G Kwiecinski, S. C. Pedersen, F. Simal, and R. J. Baker. 2012b. Evolutionary history of Caribbean species of *Myotis*, with evidence of a third Lesser Antillean endemic. Mammalian Biology 77:124-134.

Lindgreen, S. 2012. AdapterRemoval: easy cleaning of next-generation sequencing reads. BMC Research Notes 5:337-337.

López -González, C., S. J. Presley, R. D. Owen, M.R. Willig. 2001. Taxonomic status of *Myotis* (Chiroptera: Vespertilionidae) in Paraguay. Journal of Mammalogy 82:138-160.

Mak, S. S. T., S. Gopalakrishnan, C. Carøe, C. Geng, S. Liu, M. H. S. Sinding, L. F. K. Kuderna, W. Zhang, S. Fu, F. G. Vieira, M. Germonpre, H. Bocherens, S. Fedorov, B. Petersen, T. Sicheritz-Ponten, T. Marques-Bonet, G. Zhang, H. Jiang, and M.T.P. Gilbert. 2017. Comparative performance of the BGISEQ-500 vs Illumina HiSeq2500 sequencing platforms for palaeogenomic sequencing. Gigascience 6:1-13.

Mammal Diversity Database. 2020. www.mammal.diversity.org. American Society of Mammalogist. Accessed 2020-04-19.

Mantilla-Meluk, H., and J. Munoz-Garay. 2014. Biogeography and taxonomic status of *Myotis keaysi pilosatibialis* LaVal 1973 (Chiroptera: Vespertilionidae). Zootaxa 3793:60-70.

Matthee, C. A., and S. K. Davis. 2001. Molecular insights into the evolution of the family Bovidae: A nuclear DNA perspective. Molecular Biology and Evolution 18:1220-1230.

McLean, B. S., D. J, Jackson, and J. A. Cook. 2016. Rapid divergence and gene flow at high latitudes shape the history of Holarctic ground squirrels (*Urocitellus*). Molecular Phylogenetics and Evolution 102:174-188.

Meng, G., Y. Li, C. Yang, and S. Liu. 2019 MitoZ: a toolkit for animal mitochondrial genome assembly, annotation and visualization. Nucleic Acids Research 47:1-7.

Moratelli, R., and Wilson, D. 2011. A new species of *Myotis* Kaup, 1829 (Chiroptera: Vespertilionidae) from Ecuador. Mammalian Biology 76:608-614.

Moratelli, R., A. L. Gardner, J. A. De Oliveira, and D. E. Wilson. 2013. Review of *Myotis* (Chiroptera, Vespertilionidae) from northern South America, including description of a new species. American Museum Novitates:1-36.

Moratelli, R., and D. E. Wilson. 2014. A new species of *Myotis* (Chiroptera, Vespertilionidae) from Bolivia. Journal of Mammalogy 95:17-25.

Moratelli, R., D. E. Wilson, A. L. Gardner, R. D. Fisher, and E. E. Gutierrez. 2016. A New Species of *Myotis* (Chiroptera: Vespertilionidae) from Suriname. Pp 49-66 in Contributions in Natural History: A memorial Volume in Honor of Clyde Jones (Manning, R, Goetze, J.R and Yancey II, F.D). Special Publications Nº 65, Museum of Texas Tech University, Lubbock, EE.UU.

Moratelli, R., D. E. Wilson, R. L. M. Novaes, K. M. Helgen, and E. E. Gutierrez. 2017. Caribbean *Myotis* (Chiroptera, Vespertilionidae), with description of a new species from Trinidad and Tobago. Journal of Mammalogy 98:994-1008.

Morrone, J. J. 2017**.** Neotropical Biogeography: Regionalization and Evolution. CRC Press Taylor & Francis Group, Boca Raton, FL, EE.UU.

Naidu, A., R. R. Fitak, A. Munguia-Vega, and M. Culver. 2012. Novel primers for complete mitochondrial cytochrome b gene sequencing in mammals. Molecular Ecology Resources 12:191-196.

Nguyen, L. T., H. A. Schmidt, A. von Haeseler, and B. Q. Minh. 2015. IQ-TREE: A Fast and Effective Stochastic Algorithm for Estimating Maximum-Likelihood Phylogenies. Molecular Biology and Evolution 32:268-274.

Patterson, B. D., P. W. Webala, J. C. K. Peterhans, S. M. Goodman, M. Bartonjo, and T. C. Demos. 2019. Genetic variation and relationships among Afrotropical species of *Myotis* (Chiroptera: Vespertilionidae). Journal of Mammalogy 100:1130-1143.

Queiroz de, K. 2007. Species Concepts and Species Delimitation. Systematic Biology 56:879-886.

R Core Team. 2020. R: A language and environment for statistical computing. R Foundation for Statistical Computing, Vienna , Austria. URL http://www.R-project.org/.

Rambaut, A., A. J. Drummond, D. Xie, G. Baele, and M. A. Suchard. 2018. Posterior Summarization in Bayesian Phylogenetics Using Tracer 1.7. Systematic Biology 67:901-904.

Revelle, W. 2020. Psych: Procedures for Psychological, Psychometric, and Personality Research. Northwestern University, Evanston, Illinois. R package version 2.0.7.

Ridgway, R. 1912. Color standards and color nomenclature. Available at Biodiversity Heritage Library (www.biodiversitylibrary.org).

Rice, W. R. 1989. Analyzing tables of statistical test. Evolution 43:223-225. 01-904.

Rodriguez, R. M., and L. K. Ammerman. 2004. Mitochondrial DNA divergence does not reflect morphological difference between *Myotis californicus* and *Myotis ciliolabrum*. Journal of Mammalogy 85:842-851.

Roehrs, Z. P., J. B. Lack, and R. A. Van den Bussche. 2010. Tribal phylogenetic relationships within Vespertilioninae (Chiroptera: Vespertilionidae) based on mitochondrial and nuclear sequence data. Journal of Mammalogy 91:1073-1092.

Ronquist, F., M. Teslenko, P.Van der Mark, D.L, Ayres, A. Darling, S. Höhna, B. Larget, L. Liu, M. A, Suchard, and J. Huelsenbeck. 2012. MrBayes 3.2: Efficient Bayesian Phylogenetic Inference and Model Choice Across a Large Model Space. Systematic Biology 61:539-542.

Ruedi, M., and F. Mayer. 2001. Molecular systematics of bats of the genus *Myotis* (vespertilionidae) suggests deterministic ecomorphological convergences. Molecular Phylogenetics and Evolution 21:436-448.

Ruedi, M., B. Stadelmann, Y. Gager, E. J. P. Dourezy, C. M. Francis, L-K. Lin, A. Guillén-Servent, and A. Cibois . 2013. Molecular phylogenetic reconstructions identify East Asia as the cradle for the evolution of the cosmopolitan genus *Myotis* (Mammalia, Chiroptera). Molecular Phylogenetics and Evolution 69:437-449.

Salicini, I., C. Ibanez, and J. Juste. 2011. Multilocus phylogeny and species delimitation within the Natterer's bat species complex in the Western Palearctic. Molecular Phylogenetics and Evolution 61:888-898.

Schubert, M., S. Lindgreen, and L. Orlando. 2016. AdapterRemoval v2: rapid adapter trimming, identification, and read merging. BMC Research Notes 9:88-88.

Sikes, R. S., and M. Anim Care Use Comm Amer Soc. 2016. Guidelines of the American Society of Mammalogists for the use of wild mammals in research and education. Journal of Mammalogy 97:663-688.

Swofford, D. L. (2003). PAUP*. Phylogentic analysis using parsimony (* and other methods). Version 4.0a168. Sinauer Associates, Sunderland.

Stadelmann, B., L. G. Herrera, J. Arroyo-Cabrales, J. J. Flores-Martinez, B. P. May, and M. Ruedi. 2004. Molecular systematics of the fishing bat *Myotis* (*Pizonyx*) *vivesi*. Journal of Mammalogy 85:133-139.

Stadelmann, B., L. K. Lin, T. H. Kunz, and M. Ruedi. 2007. Molecular phylogeny of New World *Myotis* (Chiroptera, Vespertilionidae) inferred from mitochondrial and nuclear DNA genes. Molecular Phylogenetics and Evolution 43:32-48.

Stephens, M., N. J. Smith, and P. Donnelly. 2001. A new statistical method for haplotype reconstruction from population data. American Journal of Human Genetics 68:978-989.

Trifinopoulos, J., L. T. Nguyen, A. von Haeseler, and B. Q. Minh. 2016. W-IQ-TREE: a fast online phylogenetic tool for maximum likelihood analysis. Nucleic Acids Research 44:232-235.

Venables, W. N., and Ripley, B. D. 2002. Modern Applied Statistics with S. Springer, New York, EE.UU.

Valencia, R., C. Cerón, W. Palacios, and R. Sierra. 1999. Las formaciones naturales de la Sierra del Ecuador. Pp. 79-108 *in* Propuesta Clasificación de Vegetación para el Ecuador Contiental (Sierra, R., eds.). Quito, Ecuador: Proyecto INEFAN/GEF-BIRF and EcoCiencia.

Voss, R. S., B. K. Lim, J. F. Diaz -Nieto, and S. A. Jansa. 2013. A New Species of *Marmosops* (Marsupialia: Didelphidae) from the Pakaraima Highlands of Guyana, with Remarks on the Origin of the Endemics Pantepui Mammal Fauna. American Museum Novitates 3778:1-27.

Wickham, H. 2016. ggplot2: Elegant Graphics for Data Anlyses. Springer-Verlag, New York, EE.UU.

Wilson, D. E. 2008. [2007]. Genus *Myotis*. Pp. 468-481 in Mammals of South America, Volume I Marsupials, Xenarthrans, Shrews and Bats (Gardner, A.L, ed). The University of Chicago Press, Chicago, EE.UU.

Zar, J. H. 1998. Biostatistical analysis (4th ed). Upper Saddle River, NJ: Prentice Hall.

Associated editor: Jorge Salazar-Bravo
Submitted: April 20, 2020; Reviewed: June 23, 2020;
Accepted: September 20, 2020; Published on line: September 30, 2020.

Appendix 1. Specimens examined in morphological and morphometric analysis. Specimens are organized according to taxa herein recognized. These vouchers consist of fluid preserved specimens, stuffed skins, and skulls deposited in the following institutions: American Museum of Natural History (AMNH); Field Museum of Natural History (FMNH); Natural History Museum, University of Kansas (KU); Natural History Museum of Los Angeles County, Los Angeles, (LACM); Louisiana State University Museum of Natural Science, Baton Rouge (LSUMZ); Museum of Vertebrate Zoology, University of California, Berkeley (MVZ); Museum of Southwestern Biology, University of New Mexico (MSB); National Museum of Natural History, Smithsonian Institution (USNM); Museo de Zoología, División de Mastozoología, Pontificia Universidad Católica del Ecuador (QCAZ), Royal Ontario Museum (ROM); Sam Noble Oklahoma Museum of Natural History, University of Oklahoma (SNOMNH); Texas A&M Biodiversity Research and Teaching Collection, College Station (TCWC); Museum of Texas Tech University (TTU). Localities are arranged alphabetically by species and major political units. Specimens marked with asterisks were included in the principal component and discriminant analyses.

Myotis albescens. ARGENTINA (*n* = 1): Tucumán, Trancas, km 42 on Hwy 364, S San Pedro de Colalao (SNOMNH 23790). PERU (*n* = 7): Uyacali, Balta, Río Curanja (MSB 28518-24).

Myotis armiensis sp. n. PANAMA (*n* = 16): Chiriquí, Bugaba, La Amistad International Park, Rangers Station (MSB 262089* [holotype], MSB 262085, MSB 262237 [paratypes]); Chiriquí, Bugaba, Renacimiento, Jurutungo, Río Sereno, La Amistad International Park (MSB 262788 [paratype]), Chiriquí, Renacimiento, Santa Clara (TTU 39146 [paratype]), Chiriquí, Renacimiento, Santa Clara, Ojo de Agua, 2 km N of Santa Clara (ROM 104302 [paratype]), Chiriquí, Tierras Altas, Cerro Punta, Casa Tiley (USNM 323599* [paratype]), Chiriquí, Tierras Altas, El Volcán 2 min SW (USNM 331942*, USNM 331943* [paratypes]), Chiriquí, Bugaba, 36 Km, North of Concepción (TCWC 12655-59* [paratypes]); ECUADOR (*n* = 3): Tungurahua Province, Azuay (TTU 85060 [paratype]), Napo Province, Cosanga, Cabañas del Aliso (QCAZ 17245 [paratype]), Zamora Chinchipe, Yantzaza, Campo Minero Fruta del Norte (QCAZ 12461[paratype]).

Myotis chiloensis. ARGENTINA (*n* = 1): 19 km N Villa La Angostura along Hwy 234 (SNOMNH 23496).

Myotis diminutus. ECUADOR (*n* = 1): Los Ríos, Rio Palenque Science Center. 47 km S (by road) of Santo Domingo de los Colorados (USNM 528569 [holotype]).

Myotis dinellii. ARGENTINA (*n* = *2*): Salta, Guachipas, 7.8 km NNE Pampa Grande along Ruta Provincial 6 along Rio Cachi (SNOMNH 27933), Chubut, 3 km N Tecka along Hwy 40 (SNOMNH 23497).

Myotis keaysi. BOLIVIA (*n* = 1): Cochabamba Jachá Suyu (MSB 70381); PERU (*n* = 5): Puno Ocaneque, 10 mi N Limbani (MVZ 116050*); Cuzco, Cordillera Vilcabamba (AMNH 236134*, 233857*, 233854*, 214371*).

Myotis levis. BRASIL (*n* = 1): Sao Paulo, Estación Biológica Boraceia (FMNH 145327).

Myotis nigricans. BRASIL (*n* = 3) km 42 Antigua Rodavia Río-Sao Paulo. Iguatari Municipality, Rio de Janeiro (TCWC 22811-13 [neotypes]).

Myotis oxyotus oxyotus. ECUADOR (*n* = 3): Carchi, Gruta Rumichaca, 2 mi E La Paz (TCWC 12703-04, TCWC 12706 [neotypes]). PERU (*n* = 4) Huánuco, 10 Km N. Acomayo Bosque Unchog (MSB 49971-72); Huánuco 9 min S Huánuco (TCWC 12710-11).

Myotis oxyotus gardneri. COSTA RICA (*n* = 3) San José, Fila la Máquina (LSUMZ 12924* [holotype], 12917*,12929*). PANAMA (*n* = 3) Cerro Punta (USNM 318386*), Finca Lara (USNM 318869*, 318870*).

Myotis pilosatibialis. EL SALVADOR (*n* = 6) Ahuachapán, El Imposible, San Francisco Méndez (ROM 101273*), Santa Ana, Parque Nacional Montecristo, Bosque Nebuloso (ROM 101352*, 101357*, 101430*), Santa Ana, Parque Nacional Montecristo, Los Planes (ROM 101467*), Santa Ana, Hacienda Escuintla (TTU 60981*). HONDURAS (*n* = 7): Francisco Morazán, 1 km W of Talanga (LACM 36879* [holotype], TCWC 24101-24105 [paratypes]); Cortés, Omoa, 5.5 km southeast of Cuyamel, Santo Domingo (AMNH 265126). GUATEMALA (3): Petén Department, 12 km of Chinaja (KU 82105, 82108, 82109). MEXICO (*n* = 1): San Luis Potosí (TTU 35360*).

Myotis riparius. BOLIVIA (*n* = 1): Cochabamba, Sajta (MSB 70383); ARGENTINA (*n* = 1): Tucumán, Tafí Viejo. 5 km S.W. Siambon (SNOMNH 36220). ECUADOR (*n* = 1): Esmeraldas, Comuna San Francisco de Bogotá (TTU 102833). PARAGUAY (*n* = 1): Department of Canindeyu, Reserva Natural Privada Itabo (TTU 99378).

Myotis sp. MEXICO (*n* = 4) Yucatán Peninsula, Quintana Roo, Pueblo Nuevo (KU 91911*, KU 91912*, KU 91915*, KU 91916*).

Appendix 2. List of specimens used in cytochrome-*b* analyses of Neotropical *Myotis*. Specimens details, localities, and Genbank accession numbers of sampled individuals of Neotropical *Myotis*. Carnegie Museum of Natural History (CM); France (Catzeflis-Montpellier-V-); Field Museum of Natural History (FMNH); Jean-François Maillard (JFM DIREN); Kunico Kawai (KK); Museum National Histoire Naturelle (MNHN); The Angeles County Museum of Natural History (LACM); Museum of Vertebrate, Zoology, University of California Berkeley (MVZ); Museum of Southwestern Biology, The University of New Mexico (MSB); National Museum Prague (NMP); Osaka City University Graduate School of Medicine (OCUMS); Museo de Zoología de la Pontificia Universidad Católica del Ecuador (QCAZ); T.H. Kunz (THK); Museum of Texas Tech University (TTU and TK); Universidad Autónoma Metropolitana-Iztapalapa (UAMI); University of Nebraska State Museum (UNSM).

Institution	Cat. No.	Species	GenBank	Country	Locality	Latitude	Longitude	Source
CM	63920	*Myotis albescens*	JX130444	Suriname	Nickerie	5.63	-56.79	Larsen *et al.* (2012a)
TTU	85088	*Myotis albescens*	JX130463	Ecuador	Pastaza	-1.44	-77.99	Larsen *et al.* (2012a)
TTU	85089	*Myotis albescens*	JX130464	Ecuador	Pastaza	-1.44	-77.99	Larsen *et al.* (2012a)
TTU	102363	*Myotis albescens*	JX130472	Ecuador	El Oro	-3.51	-80.13	Larsen *et al.* (2012a)
TTU	102348	*Myotis albescens*	JX130500	Ecuador	El Oro	-3.51	-80.13	Larsen *et al.* (2012a)
TTU	103744	*Myotis albescens*	JX130501	Ecuador	Guayas	-2.45	-79.62	Larsen *et al.* (2012a)
TK	151814	*Myotis albescens*	JK130586	Ecuador	Zamora-Chinchipe	----	----	Larsen *et al.* (2012a)
FMNH	162543	*Myotis albescens*	AF376839	Bolivia	Tarija	-21.78	-64.09	Ruedi and Mayer (2001)
FMNH	174926	*Myotis albescens*	MK799657	Perú	Maskoitania	-12.77	-71.38	Patterson *et al.* (2019)
TTU	46343	*Myotis albescens*	JX130445	Perú	Huánuco	-09.18	-75.59	Larsen *et al.* (2012a)
TTU	99124	*Myotis albescens*	JX130503	Paraguay	Boquerón	-21.73	-60.95	Larsen *et al.* (2012a)
TTU	99801	*Myotis albescens*	JX130502	Paraguay	Ñeembucú	-27.04	-57.86	Larsen *et al.* (2012a)
TTU	99818	*Myotis albescens*	JX130504	Paraguay	Ñeembucú	-27.04	-57.86	Larsen *et al.* (2012a)
MSB	262089	*Myotis armiensis* sp. n.	MW025265	Panamá	Chiriquí	8.89	-82.61	This study
MSB	262237	*Myotis armiensis* sp. n.	MW025266	Panamá	Chiriquí	8.89	-82.61	This study
MSB	262085	*Myotis armiensis* sp. n.	MW025268	Panamá	Chiriquí	8.89	-82.61	This study
MSB	262788	*Myotis armiensis* sp. n.	MW025267	Panamá	Chiriquí	8.89	-82.61	This study
TTU	39146	*Myotis armiensis* sp. n.	JX130435	Panamá	Chiriquí	----	----	Larsen *et al.* (2012a)
QCAZ	12461	*Myotis armiensis* sp. n.	MW025274	Ecuador	Zamora Chinchipe	-3.75	-78.53	This study
QCAZ	17245	*Myotis armiensis* sp. n.	MW025269	Ecuador	Napo	-0.62	-77.90	This study
TTU	85060	*Myotis armiensis* sp. n.	JX130514	Ecuador	Tungurahua	-1.34	-78.20	Larsen *et al.* (2012a)
MVZ	168933	*Myotis atacamensis*	AM261882	Perú	Olmos	-5.84	-79.82	Ruedi and Mayer (2001)
USNM ZM	29470	*Myotis attenboroughi*	JN020573	Tobago	St. George Parish	11.32	-60.55	Larsen *et al.* (2012b)
THK	002	*Myotis austroriparius*	AM261885	United States	Tennessee	35.51	-86.58	Stadelmann *et al.* (2007)
THK	I	*Myotis chiloensis*	AM261888	Chile	Santiago de Chile	-33.44	-70.66	Stadelmann *et al.* (2007)
TTU	109227	*Myotis clydejonesi*	JX130520	Suriname	Sipaliwini	4.43	56.12	Larsen *et al.* (2012a)
UAMI -TK (R. Lopez-Wilchis)	45364	*Myotis fortidens*	JX130439	México	Michoacán	----	----	Larsen *et al.* (2012a)
UAMI -TK (R. Lopez-Wilchis)	43134	*Myotis fortidens*	JX130437	México	Michoacán	----	----	Larsen *et al.* (2012a)
LACM	3713/ LAF0030	*Myotis fortidens*	KC747690	México	Guerrero	----	----	Patrick & Stevens (2014)
THK	11500	*Myotis grisescens*	AM261892	USA	Tennessee	35.51	-86.58	Stadelmann *et al.* (2007)
TTU	48161	*Myotis* cf. *handleyi*	JN020569	Venezuela	Guárico	8.56	-67.57	Larsen *et al.* (2012b)
TTU	48170	*Myotis* cf. *handleyi*	JX130544	Venezuela	Guárico	8.56	-67.57	Larsen *et al.* (2012a)
TTU	48163	*Myotis* cf. *handleyi*	JX130531	Venezuela	Guárico	8.56	-67.57	Larsen *et al.* (2012a)
TTU	48164	*Myotis* cf. *handleyi*	JX130532	Venezuela	Guárico	8.56	-67.57	Larsen *et al.* (2012a)
TTU	48168	*Myotis* cf. *handleyi*	JX130533	Venezuela	Guárico	8.56	-67.57	Larsen *et al.* (2012a)
CM	78645	*Myotis* cf. *handleyi*	JX130535	Venezuela	Guárico	----	----	Larsen *et al.* (2012a)
TTU	48169	*Myotis* cf. *handleyi*	JX130543	Venezuela	Guárico	8.56	-67.57	Larsen *et al.* (2012a)
TTU	48166	*Myotis* cf. *handleyi*	JX130494	Venezuela	Guárico	8.56	-67.57	Larsen *et al.* (2012a)
QCAZ	11383	*Myotis keaysi*	JX130517	Ecuador	Chimborazo	----	----	Larsen *et al.* (2012a)
QCAZ	11380	*Myotis keaysi*	JX130516	Ecuador	Chimborazo	----	----	Larsen *et al.* (2012a)
MSB	70381	*Myotis keaysi*	MW025273	Bolivia	Cochabamba	-17.21	-65.86	This study
MVZ	185681	*Myotis lavali*	AF376864	Brazil	Paraiba	-7.11	-34.86	Ruedi and Mayer (2001)

FMNH	141600	*Myotis levis*	AF376853	Brazil	São Paulo	-23.53	-45.84	Ruedi and Mayer (2001)
MNHN	2005-895	*Myotis martiniquensis*	JN020557	Martinique, France	Grand' Rivière, Martinique	-14.87	-61.17	Larsen *et al.* (2012b)
V	2352	*Myotis martiniquensis*	JN020559	Martinique, France	Grand' Rivière, Martinique	-14.87	-61.17	Larsen *et al.* (2012b)
MNHN	2008-974	*Myotis martiniquensis*	JN020560	Martinique, France	Grand' Rivière, Martinique	-14.87	-61.17	Larsen *et al.* (2012b)
V	2354	*Myotis martiniquensis*	JN020561	Martinique, France	Grand' Rivière, Martinique	-14.872	-61.17	Larsen *et al.* (2012b)
JFM	DIREN 2	*Myotis martiniquensis*	AM262332	Martinique France	----	----	----	Stadelmann *et al.* (2007)
CM	98859	*Myotis* cf. *nigricans*	JX130453	Perú	Huánuco	-----	----	Larsen *et al.* (2012a)
CM	77691	*Myotis* cf. *nigricans*	JX130497	Suriname	Marowijne	----	----	Larsen *et al.* (2012a)
No voucher	-----	*Myotis nesopolus*	JN20575	Netherlands, Antilles	Bonaire	12.201	-68.26	Larsen *et al.* (2012b)
No voucher	-----	*Myotis nesopolus*	JN20577	Netherlands, Antilles	Bonaire	12.201	-68.26	Larsen *et al.* (2012b)
CM	83427	*Myotis nyctor*	JN020562	Grenada	St. David Parish	----	----	Larsen *et al.* (2012b)
TTU	109225	*Myotis nyctor*	JN020563	Barbados	St. Thomas Parish	13.19	-59.57	Larsen *et al.* (2012b)
TTU	109229	*Myotis nyctor*	JN020565	Barbados	St. Thomas Parish	13.20	-59.53	Larsen *et al.* (2012b)
TTU	109230	*Myotis nyctor*	JN020567	Barbados	St. Thomas Parish	13.14	-59.60	Larsen *et al.* (2012b)
FMNH	129208	*Myotis oxyotus*	AF376865	Perú	Lima	----	----	Ruedi and Mayer (2001)
TTU	35360	*Myotis pilosatibialis*	JX130526	México	San Luis Potosí	22.00	-99.00	Larsen *et al.* (2012a)
TTU	35631	*Myotis pilosatibialis*	JX130518	México	San Luis Potosí	22.00	-99.00	Larsen *et al.* (2012a)
TTU	60981	*Myotis pilosatibialis*	JX130519	San Salvador	Santa Ana	13.46	-88.88	Larsen *et al.* (2012a)
MVZ	226976	*Myotis pilosatibialis*	MW025271	Guatemala	Alta Verapaz	15.61	-90.27	This study
MVZ	226973	*Myotis pilosatibialis*	MW025272	Guatemala	El Quiche	15.46	-90.78	This study
MVZ	224798	*Myotis pilosatibialis*	MW025275	Guatemala	Quetzaltenango	14.74	-91.47	This study
MVZ	AD199	*Myotis riparius*	AF376866	Brazil	Pernambuco	----	----	Ruedi and Mayer (2001)
CM	78651	*Myotis riparius*	JX130490	Venezuela	----	----	----	Larsen *et al.* (2012a)
CM	78659	*Myotis riparius*	JX130474	Venezuela	Bolívar	----	----	Larsen *et al.* (2012a)
TTU	99378	*Myotis riparius*	JX130491	Paraguay	Canindeyú, Paraguarí	-24.46	-54.66	Larsen *et al.* (2012a)
CM	68443	*Myotis riparius*	JX130473	Suriname	Paramaribo	----	----	Larsen *et al.* (2012a)
Voucher 3011	----	*Myotis* cf. *riparius*	AM261891	Costa Rica	La Selva	----	----	Stadelmann *et al.* (2007)
TTU	85344	*Myotis riparius*	JX130469	Ecuador	Esmeraldas	1.23	-78.76	Larsen *et al.* (2012a)
TTU	85345	*Myotis riparius*	JX130515	Ecuador	Esmeraldas	1.23	-78.76	Larsen *et al.* (2012a)
TTU	102883	*Myotis riparius*	JX130492	Ecuador	Esmeraldas	1.09	-78.70	Larsen *et al.* (2012a)
TK	22703	*Myotis riparius*	JX130436	Perú	Huánuco	----	----	Larsen *et al.* (2012a)
THKMys	ET3	*Myotis riparius*	AM262336	Brazil	----	----	----	Stadelmann *et al.* (2007)
TTU	85090	*Myotis riparius*	TK104318	Ecuador	Pastaza	-1.46	-78.10	Larsen *et al.* (2012a)
TTU	122454	*Myotis riparius*	JX130448	Paraguay	Canindeyú	-23.98	-55.36	Larsen *et al.* (2012a)
MVZ	185999	*Myotis ruber*	AF376867	Brazil	Salesopolis	-22.16	-48.75	Ruedi and Mayer (2001)
UAMI	15305	*Myotis velifer*	JX130589	México	Michoacán	----	----	Larsen *et al.* (2012a)
UAMI	15306	*Myotis velifer*	JX130438	México	Michoacán	----	----	Larsen *et al.* (2012a)
MVZ	146766	*Myotis velifer*	AF376870	México	Michoacán	27.06	-109.01	Stadelmann *et al.* (2007)
UAMI	15304	*Myotis velifer*	JX130462	México	Michoacán	----	----	Larsen *et al.* (2012a
TTU	110032	*Myotis velifer*	JX130582	México	Tamaulipas	24.01	-98.34	Larsen *et al.* (2012a)
TTU	44818	*Myotis velifer*	EU680299	México	Tamaulipas	----	----	Parlos *et al.* (2008) Unpublished
TTU	43197	*Myotis velifer*	AY460343	USA	Oklahoma	----	----	Rodriguez and Ammerman (2004)
CS -H	TK 46327	*Myotis velifer*	JX130592	México	Michoacán	----	----	Larsen *et al.* (2012a)
TK	48587	*Myotis velifer*	EF222340	USA	Texas	----	----	Baird *et al.* (2008)
TTU	44816	*Myotis velifer*	JX130478	México	Tamaulipas	----	----	Larsen *et al.* (2012a)
TTU	60983	*Myotis velifer*	JX130477	San Salvador	Santa Ana	----	----	Larsen *et al.* (2012a)
TTU	109261	*Myotis velifer*	JX130468	USA	Texas	29.50	-103.43	Larsen *et al.* (2012a)
No voucher	----	*Myotis vivesi*	AJ504406	México	Gulf of California	28.52	113.02	Stadelmann *et al.* (2004)

MVZ	155853	*Myotis yumanensis*	AF376875	USA	California	38.04	-122.80	Stadelmann *et al.* (2007)
CM	77691	*Myotis* cf. *nigricans*	JX130497	Suriname	Marowijne	----	----	Larsen *et al.* (2012a)
TTU	47514	*Myotis* sp.	JX130449	México	Yucatán	ca.20.96	ca. -89.59	Larsen *et al.* (2012a)
JAG	286	*Myotis* sp.	JX130525	México	Yucatán	----	----	Larsen *et al.* (2012a)
TK	13532	*Myotis* sp.	AF376852	México	Yucatán	----	----	Ruedi and Mayer (2001)
CM	55764	*Myotis* sp.	JX130489	México	Vera Cruz	----	----	Larsen *et al.* (2012a)
MVZ	226977	*Myotis* sp.	MW025270	Guatemala	Alta Verapaz	15.61	-90.27	This study
CM	77705	*Myotis* sp	JX130505	Suriname	Paramaribo	----	----	Larsen *et al.* (2012a)
TTU	61228	*Myotis* sp	JX1304931	Honduras	Valle	13.30	-87.49	Larsen *et al.* (2012a)
TTU	102707	*Myotis* sp	JX130471	Ecuador	Oro	-3.87	-80.09	Larsen *et al.* (2012a)
TTU	46348	*Myotis* sp	JX130481	Perú	Huánuco	----	----	Larsen *et al.* (2012a)
				Outgroups				
NMPPB	916	*Myotis brandtii*	AM261886	Russia	N-W. Russia	----	----	Stadelmann *et al.* (2007)
Mgf	----	*Myotis gracilis*	AB243030	Japan	Hokkaido	----	----	Kawai *et al.* (2006)
MgE	----	*Myotis gracilis*	AB243029	Japan	Hokkaido	----	----	Kawai *et al.* (2006)
OCUMS	5362	*Myotis gracilis*	AB106605	Japan	Hokkaido	----	----	Kawai *et al.* (2003)
KK	0005	*Myotis yanbarensis*	AB106610	Japan	Hokkaido	----	----	Kawai *et al.* (2003)

Appendix 3. List of specimens used in cytochrome oxidase *c* subunit I analyses of Neotropical *Myotis*. Specimens details, localities, and Genbank accession numbers of sampled individuals of Neotropical *Myotis*. Field Museum of Natural History (FMNH); Museum of Vertebrate, Zoology, University of California Berkeley (MVZ); Museum of Southwestern Biology, The University of New Mexico (MSB); Museum of Texas Tech University (TTU and TK); Royal Ontario Museum (ROM); Zoological Museum of Moscow State University (ZMMU).

Institution	Cat. No./Sequence Code	Species	GenBank	Country	Locality	Lat.	Long.	Source
ROM	120231	*Myotis albescens*	HQ545684	Suriname	Sipaliwini	1.94	-56.06	Lim *et al.* (unpubl.)
TTU	85060	*Myotis armiensis* sp. n.	MW042013	Ecuador	Tungurahua	-1.34	-78.2	This study
MSB	262788	*Myotis armiensis* sp. n.	MW042014	Panamá	Las Nubes Ranger Station, Parque Internacional La Amistad	8.89	-82.61	This study
No voucher	Mke140204.2.VS	*Myotis armiensis* sp. n.	KX814396	Costa Rica	Valle del Silencio, Parque Internacional La Amistad	9.10	-82.96	Chaverri *et al*. (2016)
No voucher	Mke140204.4.VS	*Myotis armiensis* sp. n.	KX814397	Costa Rica	Valle del Silencio, Parque Internacional La Amistad	9.10	-82.96	Chaverri *et al*. (2016)
No voucher	Mke140204.5.VS	*Myotis armiensis* sp. n.	KX814398	Costa Rica	Valle del Silencio, Parque Internacional La Amistad	9.10	-82.96	Chaverri *et al*. (2016)
No voucher	Mke140204.8.VS	*Myotis armiensis* sp. n.	KX814399	Costa Rica	Valle del Silencio, Parque Internacional La Amistad	9.10	-82.96	Chaverri *et al*. (2016)
No voucher	Mke150126.1.VS	*Myotis armiensis* sp. n.	KX814400	Costa Rica	Valle del Silencio, Parque Internacional La Amistad	9.08	-82.97	Chaverri *et al*. (2016)
No voucher	Mke150201.18.VS	*Myotis armiensis* sp. n.	KX814403	Costa Rica	Valle del Silencio, Parque Internacional La Amistad	9.11	-82.96	Chaverri *et al*. (2016)
No voucher	Mke140128.1.VS	*Myotis armiensis* sp. n.	KX814393	Costa Rica	Valle del Silencio, Parque Internacional La Amistad	9.10	-82.96	Chaverri *et al*. (2016)
No voucher	Mke150126.3.VS	*Myotis armiensis* sp. n.	KX814401	Costa Rica	Valle del Silencio, Parque Internacional La Amistad	9.08	-82.97	Chaverri *et al*. (2016)
No voucher	Mke140129.1.VS	*Myotis armiensis* sp. n.	KX814394	Costa Rica	Valle del Silencio, Parque Internacional La Amistad	9.08	-82.97	Chaverri *et al*. (2016)
No voucher	Mke140131.3.VS	*Myotis armiensis* sp. n.	KX814395	Costa Rica	Valle del Silencio, Parque Internacional La Amistad	9.11	-82.96	Chaverri *et al*. (2016)
No voucher	Mke150126.9.VS	*Myotis armiensis* sp. n.	KX814402	Costa Rica	Valle del Silencio, Parque Internacional La Amistad	9.08	-82.97	Chaverri *et al*. (2016)
ROM	104302	*Myotis armiensis* sp. n.	JF447424	Panamá	Chiriquí	8.87	-82.75	Clare *et al.* (2011)
ROM	97827	*Myotis nigricans*	JQ601557	Guyana	Kuma River	3.26	-59.71	Engstrom *et al.* (unpubl.)
ROM	106737	*Myotis nigricans*	JQ601572	Guyana	Essequibo River	1.58	-58.63	Lim *et al.* (unpubl.)
ROM	106772	*Myotis nigricans*	JQ601574	Guyana	Gunn´s Strip	1.65	-58.63	Lim *et al.* (unpubl.)

ROM	F43329	*Myotis nigricans*	JQ601579	Guyana	Paruima	5.81	-61.06	Lim *et al.* (unpubl.)
ROM	105148	*Myotis nigricans*	JQ601611	Ecuador	Parque Nacional Yasuní	-0.63	-76.45	Engstrom *et al.* (unpubl.)
ROM	118840	*Myotis nigricans*	JQ601620	Ecuador	Orellana	-0.68	-76.43	Reid *et al.* (unpubl.)
ROM	114671	*Myotis nigricans*	JQ601582	Guyana	Mount Ayanganna	5.33	-53.91	Lim *et al.* (unpubl.)
ROM	98018	*Myotis nigricans*	EF080493	Guyana	Potaro-Sirapurini	4.38	-58.37	Clare *et al.* (2007)
ROM	117431	*Myotis nigricans*	EU096808	Suriname	Sipaliwini	4.54	-56.93	Borisenko *et al.* (2008)
No voucher	Mni150205.28.VS	*Myotis nigricans*	KX814404	Costa Rica	Valle del Silencio, Parque Internacional la Amistad	9.13	-82.95	Chaverri *et al.* 2016
FMNH	174938	*Myotis oxyotus*	JN847707	Perú	Cusco, La Esperanza	-13.17	-71.60	Taylor *et al.* (2011)
MVZ	174408	*Myotis oxyotus gardneri*	MW042015	Costa Rica	Refugio Nacional Tapanti, Cartago	9.69	-83.78	This study
No voucher	Mox140201.4.VS	*Myotis oxyotus gardneri*	KX814406	Costa Rica	Valle del Silencio, Parque Internacional La Amistad	9.11	-82.96	Chaverri *et al.* (2016)
No voucher	Mox140204.6.VS	*Myotis oxyotus gardneri*	KX814409	Costa Rica	Valle del Silencio, Parque Internacional La Amistad	9.10	-82.96	Chaverri *et al.* (2016)
No voucher	Mox140201.5.VS	*Myotis oxyotus gardneri*	KX814407	Costa Rica	Valle del Silencio, Parque Internacional La Amistad	9.11	-82.96	Chaverri *et al.* (2016)
No voucher	Mox140131.1.VS	*Myotis oxyotus gardneri*	KX814405	Costa Rica	Valle del Silencio, Parque Internacional La Amistad	9.11	-82.96	Chaverri *et al.* (2016)
No voucher	Mox140204.1.VS	*Myotis oxyotus gardneri*	KX814408	Costa Rica	Valle del Silencio, Parque Internacional La Amistad	9.10	-82.96	Chaverri *et al.* (2016)
No voucher	Mox150125.2.VS	*Myotis oxyotus gardneri*	KX814410	Costa Rica	Valle del Silencio, Parque Internacional La Amistad	9.11	-82.96	Chaverri *et al.* (2016)
No voucher	Mox150125.3.VS	*Myotis oxyotus gardneri*	KX814411	Costa Rica	Valle del Silencio, Parque Internacional La Amistad	9.11	-82.96	Chaverri *et al.* (2016)
No voucher	Mox150126.10.VS	*Myotis oxyotus gardneri*	KX814412	Costa Rica	Valle del Silencio, Parque Internacional La Amistad	9.11	-82.96	Chaverri *et al.* (2016)
MVZ	226976	*Myotis pilosatibialis*	MW042012	Guatemala	Alta Verapaz	15.61	-90.27	This study
TTU	35360	*Myotis pilosatibialis*	MW042011	México	San Luis Potosí	ca. 22.00	ca. -99.00	This study
ROM	101352	*Myotis pilosatibialis*	JF446523	El Salvador	Santa Ana	14.42	-89.37	Clare *et al.* (2011)
ROM	101433	*Myotis pilosatibialis*	JF446527	El Salvador	Santa Ana	14.42	-89.37	Clare *et al.* (2011)
ROM	101432	*Myotis pilosatibialis*	JF446528	El Salvador	Santa Ana	14.42	-89.37	Clare *et al.* (2011)
ROM	101431	*Myotis pilosatibialis*	JF446529	El Salvador	Santa Ana	14.42	-89.37	Clare *et al.* (2011)
ROM	101357	*Myotis pilosatibialis*	JF446532	El Salvador	Santa Ana	14.42	-89.37	Clare *et al.* (2011)
ROM	101356	*Myotis pilosatibialis*	JF446533	El Salvador	Sant Ana	14.42	-89.37	Clare *et al.* (2011)
ROM	101355	*Myotis pilosatibialis*	JF446535	El Salvador	Sant Ana	14.42	-89.37	Clare *et al.* (2011)
ROM	101354	*Myotis pilosatibialis*	JF446536	El Salvador	Sant Ana	14.42	-89.37	Clare *et al.* (2011)
ROM	116560	*Myotis riparius*	EF080496	Guyana	Potaro-Siparuni	5.25	-59.61	Clare *et al.* (2007)
No voucher	AZ2407	*Myotis velifer*	GU723140	USA	Arizona	----	----	Streicker *et al.* (2010)
ROM	101358	*Myotis velifer*	JF446538	El Salvador	Santa Ana	14.42	-89.37	Clare *et al.* (2011)
No voucher	AZ4490	*Myotis yumanensis*	GU723138	USA	Arizona	----	----	Streicker *et al.* (2010)
No voucher	CA49	*Myotis yumanensis*	GU723137	USA	California	----	----	Streicker *et al.* (2010)
TTU	47514	*Myotis* sp.	MW042010	México	Yucatán	ca. 20.96	ca. -89.59	This study
ROM	99232	*Myotis* sp.	JF446808	Guatemala	Petén	16.30	-89.33	Clare *et al.* (2011)
ROM	99233	*Myotis* sp.	JF446809	Guatemala	Petén	16.30	-89.33	Clare *et al.* (2011)
ROM	96463	*Myotis* sp.	JF447270	México	Yucatán, Loltun	20.25	-89.48	Clare *et al*. (2011)
ROM	FN33842	*Myotis* sp.	JF447274	México	Quintana Roo, Tulum	ca. 20.21	ca. -87.46	Clare *et al.* (2011)
ROM	FN33841	*Myotis* sp.	JF447275	México	Quintana Roo, Tulum	ca. 20.21	ca. -87.46	Clare *et al.* (2011)
			Outgroups					
No voucher	Isolate IN 90	*Myotis lucifugus*	GU723128	USA	Indiana	----	----	Streicker *et al.* (2010)
KZM	SVN 14-08	*Myotis brandtii*	JF4429261	Russia	Sakhalin Region	----	----	Kruskop *et al.* (unpubl.)
ZMMU	SVK 71-08_1	*Myotis brandtii*	JF4429271	Russia	Republic of Gorno-Altay	51.28	84.73	Kruskop *et al.* (unpubl.
ZMMU	SVK 71-08_2	*Myotis brandtii*	JF4429281	Russia	Republic of Gorno-Altay	51.28	84.73	Kruskop *et al.* (unpubl.)
ZMMU	S-171531	*Myotis brandtii*	JF4429291	Russia	Kirov Region	57.35	49.09	Kruskop *et al.* (unpubl.)

Appendix 4. List of taxonomic samples included in nuclear gene analyses of Neotropical *Myotis* with institution, catalog number, species, locality and GenBank accession numbers: American Museum of Natural History (AMNH); Carnegie Museum of Natural History (CM); Field Museum of Natural History (FMNH); Indiana State University Collection (ISUV); Museum of Southwestern Biology, The University of New Mexico (MSB); Museo de Zoología de la Pontificia Universidad Católica del Ecuador (QCAZ); Museum of Texas Tech University (TTU and TK); Universidad Autónoma Metropolitana-Iztapalapa (UAMI).

Institution	Cat. No.	Species	Locality	RAG2	PRKC1	STAT5A	THY
CM	77691	*Myotis albescens*	Suriname, Marowijne	GU328076	GU328317	GU328390	GU328460
AMNH	261790	*Myotis albescens*	Bolivia, Beni	MW042018	MW041998	MW041984	MW041970
MSB	262085	*Myotis armiensis* sp. n.	Chiriquí, Panama	MW042027	MW042008	MW041994	MW041980
QCAZ	17245	*Myotis armiensis* sp. n.	Napo, Ecuador	(not sequenced)	MW042005	MW041991	MW041977
MSB	75643	*Myotis auriculus*	New Mexico, USA	MW042019	MW041999	MW041985	MW041971
TK	79325	*Myotis californicus*	USA, Texas	GU328078	GU328319	GU328392	GU328462
TK	83155	*Myotis ciliolabrum*	USA, Texas	GU328080	GU328321	GU328394	GU328464
MSB	43105	*Myotis ciliolabrum*	Mexico, Baja California	MW042016	MW041996	MW041982	MW041968
TTU	31503	*Myotis dominicensis*	Dominica, St. Joseph Parish, Dominica	GU328081	GU328322	GU328395	GU328465
MSB	279297	*Myotis evotis*	USA, New Mexico	MW042020	MW042000	MW041986	MW041972
UAMI-TK	43186	*Myotis fortidens*	Mexico, Michoacán	GU328082	GU328323	GU328396	GU328466
TK	13532	*Myotis* sp.	Yucatán, México	GU328083	GU328324	GU328397	GU328467
FMNH	141600	*Myotis levis*	Sao Paulo, Brazil	GU328085	GU328326	GU328399	GU328469
MSB	70384	*Myotis levis*	Bolivia	MW042021	MW042001	MW041987	MW041973
FMNH	129210	*Myotis nigricans*	Amazonas, Perú	GU328088	GU328329	GU328402	GU328472
AMNH	268591	*Myotis riparius*	Paracou, French Guiana	GU328089	GU328330	GU328403	GU328473
AMNH	268649	*Myotis riparius*	Bolivia, Cochabamba	MW042022	MW042002	MW041988	MW041974
AMNH	261108	*Myotis riparius*	Bolivia, Chuquisaca	MW042024	MW042004	MW041990	MW041976
ISUV 6454 -DWS	6454	*Myotis septentrionalis*	USA, Indiana	GU328090	GU328331	GU328404	GU328474
TTU	79330	*Myotis thysanodes*	USA, Texas	GU328091	(not sequenced)	(not sequenced)	GU328475
TTU	78599	*Myotis velifer*	USA, Texas	AY141033	GU328333	GU328406	GU328476
MSB	53789	*Myotis velifer*	Mexico, Sonora	MW042023	MW042003	MW041989	MW041975
TTU	79545	*Myotis volans*	USA, Texas	GU328092	GU328334	GU328407	GU328477
TTU	43200	*Myotis yumanensis*	USA, Oklahoma	GU328094	GU328336	GU328049	GU328479
MSB	42790	*Myotis* sp.	Mexico, Baja California	MW042028	MW042009	MW041995	MW041981
AMNH	268651	*Myotis keaysi*	Bolivia, Cochabamba	MW042025	MW042006	MW041992	MW041978
MSB	235490	*Myotis* cf. *nigricans*	Bolivia, Tarija	MW042026	MW042007	MW041993	MW041979
				Outgroup			
MSB	94052	*Myotis* cf. *ikonnikovi*	Mongolia, Ovorkhangai	MW042017	MW041997	MW041983	MW041969

Appendix 5. Post-hoc multiple comparison test with Bonferroni corrected approach.

Factor	Group 1	Grupo 2	Sample size group 1	Sample size group 2	Statistics	df	p	p. adj	p. adj. signif
PC1	*M. armiensis* sp. n.	*M.* sp.	10	5	1.5093	12.9886	0.155	0.31	ns
PC1	*M. armiensis* sp. n.	*M. o. gardneri*	10	6	-5.1609	13.8910	0.000148	0.001	**
PC1	*M. armiensis* sp. n.	*M. str. keaysi*	10	5	-4.1027	10.1119	0.002	0.013	*
PC1	*M.* armiensis sp. n.	*M. str. pilosatibialis*	10	8	-1.9745	9.5891	0.078	0.233	ns
PC1	*M.* sp.	*M. o. gardneri*	5	6	-8.5816	8.9647	1.29E-05	0.000129	***
PC1	*M.* sp.	*M. str. keaysi*	5	5	-6.1634	6.4085	0.000651	0.005	**
PC1	*M.* sp.	*M. str. pilosatibialis*	5	8	-5.6729	4.6410	0.003	0.015	*
PC1	*M.* o. *gardneri*	*M. str. keaysi*	6	5	0.0678	6.7613	0.948	0.948	ns
PC1	*M.* o. *gardneri*	*M. str. pilosatibialis*	6	8	6.0262	5.7218	0.001	0.008	**
PC1	M. str. keaysi	*M. str. pilosatibialis*	5	8	3.6629	4.2129	0.02	0.079	ns
PC2	*M. armiensis* sp. n.	*M.* sp.	10	5	7.4576	10.0559	2.10E-05	0.000189	***
PC2	*M. armiensis* sp. n.	*M. o gardneri*	10	6	0.7331	13.5877	0.476	0.476	ns
PC2	*M. armiensis* sp. n.	*M. str. keaysi*	10	5	2.8433	11.4061	0.016	0.062	ns
PC2	*M. armiensis* sp. n.	*M. str. pilosatibialis*	10	8	3.6824	10.5644	0.004	0.019	*
PC2	*M.* sp.	*M. o. gardneri*	5	6	-10.3063	6.5480	2.76E-05	0.000221	***
PC2	*M.* sp.	*M. str. keaysi*	5	5	-9.9125	6.7270	2.95E-05	0.000221	***
PC2	*M.* sp.	*M. str. pilosatibialis*	5	8	-9.9022	10.9032	8.76E-07	8.76E-06	****
PC2	*M. o. gardneri*	*M. str. keaysi*	6	5	3.0094	8.2366	0.016	0.062	ns
PC2	*M. o. gardneri*	*M. str. pilosatibialis*	6	8	4.3703	7.3463	0.003	0.018	*
PC2	*M. str. keaysi*	*M. str. pilosatibialis*	5	8	1.5858	8.3097	0.15	0.3	ns

Appendix 6. Molecular synapomorphies of *Myotis armiensis* sp. n, as revealed by maximum-parsimony (MP) analysis of cytochrome *c* oxidase subunit I (657 bp). Molecular transformations were optimized on a 50 % majority-rule consensus tree of the most parsimonious tree (576 steps; [CI] = 0.429) resulting from the MP analysis of the cytochrome *c* oxidase subunit I matrix. 17 fixed derived characters states were found in the newly identified lineage. Of these, 2 which are indicated by asterisks, have not evolved independently in any other species of New World *Myotis*. The remaining have appeared secondarily in at least one species of New World *Myotis*.

	Nucleotide position /Codon position	Character state in *M. armiensis* sp. n.	Characters Consistency Index
1	3/3	T	0.333
2	93/3	A	0.222
3	93/3	A	0.222
4	102/3	C	0.333
5	162/3	C	0.400
6	180/3	G	0.250
7	264/3	G	0.500
8	366/3	C	0.250
9	375/3	T	0.200
10	427/1	C	0.333
11	447/3	C	0.500
12	477/3	G	0.500
13	507/3	C	0.250
14	594/3	C	0.333
15	641/2*	A	1.000
16	646/1*	A	1.000
17	648/3	G	0.250

Appendix 7. Molecular synapomorphies of *Myotis armiensis* sp. n., as revealed by maximum-parsimony (MP) analysis of partial cytochrome *b* (~ 710 bp). Molecular transformations were optimized on a 50 % majority-rule consensus tree of the most parsimonious tree (2846 steps; [CI] = 0.238) resulting from the MP analysis of partial cytochrome *b*. 31 fixed derived characters states were found in the newly identified lineage. Of these, 1, which is indicated by asterisk, has not evolved independently in any other species of Neotropical *Myotis*. The remaining have appeared secondarily in at least one species of Neotropical *Myotis*.

	Nucleotide position /Codon position	Character state in M. armiensis sp. n.	Characters Consistency Index
1	120/3	T	0.167
2	120/3	C	0.167
3	141/3	G	0.333
4	165/3	C	0.053
5	156/3	G	0.250
6	189/3	T	0.167
7	315/3	A	0.167
8	336/3	T	0.333
9	405/3	G	0.125
10	408/3	C	0.214
11	426/3	A	0.111
12	444/3	T	0.111
13	471/3	C	0.333
14	507/3	C	0.500
15	513/3	C	0.111
16	537/3	C	0.200
17	**570/3***	**G**	**1.000**
18	603/3	T	0.167
19	678/3	C	0.167
20	697/1	T	0.200
21	723/3	C	0.200
22	741/3	C	0.154
23	744/3	T	0.143
24	756/3	C	0.077
25	759/3	C	0.125
26	765/3	C	0.100
27	780/3	C	0.100
28	798/3	C	0.100
29	804/3	C	0.100
30	813/3	G	0.100
31	822/3	T	0.143

Appendix 8. Molecular synapomorphies of *Myotis armiensis* sp. n., as revealed by maximum-parsimony (MP) analysis of protein kinase C, iota (PRKCI, *n* = 402 bp). Molecular transformations were optimized on a 50 % majority-rule consensus tree of the most parsimonious tree (59 steps; [CI] = 0.966) resulting from the MP analysis of protein kinase C, iota. All 4 fixed characters have not evolved independently in any other species of New World *Myotis*.

	Nucleotide position	Character state in M. armiensis sp. n.	Characters Consistency Index
1	29	G	1.000
2	51	C	1.000
3	240	T	1.000
4	371	G	1.000

Appendix 9. Molecular synapomorphies of *Myotis armiensis* sp. n., as revealed by maximum-parsimony (MP) analysis of signal transducer and activator of transcription 5A (STAT5A, *n* = 414 bp). Molecular transformations were optimized on a 50 % majority-rule consensus tree of the most parsimonious tree (134 steps; [CI] = 0.754) resulting from the MP analysis of signal transducer and activator of transcription 5A. 23 fixed derived characters states were found in the newly identified lineage. Of these, 9, which are indicated by asterisk, has not evolved independently in any other species of New World *Myotis*. The remaining have appeared secondarily in at least one species of New World *Myotis.*

	Nucleotide position	Character state in *M. armiensis* sp. n.	Characters Consistency Index
1	10	C	0.500
2	15	C	0.500
3	**18***	**C**	**1.000**
4	**48***	**A**	**1.000**
5	56	C	0.500
6	69	C	0.500
7	72	G	0.667
8	**99***	**C**	**1.000**
9	145	C	0.333
10	148	C	0.500
11	154	A	0.333
12	220	C	0.500
13	254	C	0.500
14	**258***	**C**	**1.000**
15	**269***	**C**	**1.000**
16	273	A	0.500
17	**276***	**C**	**1.000**
18	355	C	0.500
19	376	C	0.333
20	**391***	**T**	**1.000**
21	**393***	**G**	**1.000**
22	398	G	0.500
23	**405***	**G**	**1.000**

Appendix 10. Molecular synapomorphies of *Myotis armiensis* sp. n., as revealed by maximum-parsimony (MP) analysis of thyrotropin (THY, *n* = 475 bp). Molecular transformations were optimized on a 50 % majority-rule consensus tree of the most parsimonious tree (138 steps; [CI] = 0.906) resulting from the MP analysis of thyrotropin. 7 fixed derived characters states were found in the newly identified lineage. Of these, 6, which are indicated by asterisk, have not evolved independently in any other species of New World *Myotis*. Only one has appeared secondarily in at least one species of New World *Myotis.*

	Nucleotide position	Character state in *M. armiensis* sp. n.	Characters Consistency Index
1	**161***	**G**	**1.000**
3	**220***	**G**	**1.000**
2	**235***	**G**	**1.000**
4	**277***	**T**	**1.000**
5	**315***	**C**	**1.000**
6	**350***	**G**	**1.000**
7	373	C	0.500